

# Large-scale Retrieval for Medical Image Analytics: A Comprehensive Review

Zhongyu Li<sup>a</sup>, Xiaofan Zhang<sup>a</sup>, Henning Müller<sup>b</sup>, Shaoting Zhang<sup>a,\*</sup>

<sup>a</sup>*Department of Computer Science, University of North Carolina at Charlotte, USA*

<sup>b</sup>*University of Applied Sciences Western Switzerland (HES-SO), Sierre, Switzerland*

---

## Abstract

Over the past decades, medical image analytics was greatly facilitated by the explosion of digital imaging techniques, where huge amounts of medical images were produced with ever-increasing quality and diversity. However, conventional methods for analyzing medical images have achieved limited success, as they are not capable to tackle the huge amount of image data. In this paper, we review state-of-the-art approaches for large-scale medical image analysis, which are mainly based on recent advances in computer vision, machine learning and information retrieval. Specifically, we first present the general pipeline of large-scale retrieval, summarize the challenges/opportunities of medical image analytics on a large-scale. Then, we provide a comprehensive review of algorithms and techniques relevant to major processes in the pipeline, including feature representation, feature indexing, searching, etc. On the basis of existing work, we introduce **the evaluation protocols and** multiple applications of large-scale medical image retrieval, with a variety of exploratory and diagnostic scenarios. Finally, we discuss future directions of large-scale retrieval, which can further improve the performance of medical image analysis.

*Keywords:* Medical image analysis, information retrieval, large scale, computer aided diagnosis

---

\*Corresponding author, rutgers.shaoting@gmail.com

## 1. Introduction

Medical image analytics plays a central role in clinical diagnosis, image-guided surgery and pattern discovery. Many protocols and modalities of digital imaging techniques have been adopted to generate medical images, including magnetic resonance imaging (MRI) (Slichter, 2013), computed tomography (CT) (Hsieh, 2009), photon emission tomography (PET) (Bailey et al., 2005), ultrasound (Szabo, 2004), fluorescence microscopy (Lichtman and Conchello, 2005), X-ray (Lewis, 2004) and others. Generally, these medical images reflect specific aspects (anatomy, function) of tissue types/organs that require an accurate interpretation and analysis from either domain experts or computer-aided decision support. In comparison with domain expert analysis that is labor intensive and time-consuming, computer-aided approaches are efficient and its accuracy has increased continuously with the rapid development of computer vision, machine learning and related fields (Doi, 2014; Katouzian et al., 2012; May, 2010). To support computer-aided medical image analytics, one important task is content-based image retrieval (CBIR) (Akgül et al., 2011; Lehmann et al., 2004; Müller et al., 2004), i.e., indexing and mining images that contain a similar visual content (e.g., shape, morphology, structure, etc). For a new medical image to be analyzed, a CBIR system can first retrieve visually similar images in an existing dataset. Then, its high-level descriptions and interpretations can be explored based on the retrieved images.

Over the past 25 years, CBIR has been one of the most vivid research topics in the field of computer vision. Many CBIR methods were developed for accurate and efficient image retrieval. Especially in recent years, with the ever-increasing number of digital images (e.g., ImageNet (Russakovsky et al., 2015), COCO (Lin et al., 2014), PASCAL VOC (Everingham et al., 2010), etc), CBIR has moved towards the era of big data. Massive amounts of images can provide rich information for comparison and analysis, and thus facilitate the generation of new algorithms and techniques that can tackle image retrieval in large databases. In general, large-scale image retrieval can be divided into two stages, i.e., feature extraction to represent images and feature indexing. Deep learning (LeCun et al., 2015) is one of the most popular methods for feature representation that is particularly suitable for large image databases, where massive amounts of data can boost the retrieval performance by training deep and complex neural networks with millions of parameters (Babenko and Lempitsky, 2015; Wan et al., 2014). For the feature

38 indexing at a large-scale, the key problem is computational efficiency, i.e.,  
39 similarity searching in millions of images with thousand dimensional features  
40 vectors. Methods such as vocabulary trees (Nister and Stewenius, 2006) and  
41 hashing (Wang et al., 2016) can efficiently tackle this problem, either through  
42 changing the indexing structure or compressing the original features.

43 Despite the current large-scale methods having achieved many successes  
44 in generic image retrieval problems, how to best tackle the retrieval in large-  
45 scale medical image databases is still a very challenging topic (Zhang and  
46 Metaxas, 2016). On the one hand, the meaning of large-scale in the medical  
47 image field is somewhat different from large-scale in the generic image do-  
48 main. Generally, each patient can generate hundreds to thousands of image  
49 slices using different protocols, modalities (e.g., CT, MRI, X-ray) and multi-  
50 ple dimensions (e.g., volumetric 3D, time series). These volumes are usually  
51 stored in many single images (as slices) in the DICOM (Digitla Imaging and  
52 Communications in Medicine) format (Kahn et al., 2007). Besides this, the  
53 size of some medical images can be extremely large. For example, the whole-  
54 slide histopathological images can include more than  $100,000 \times 100,000$  pixels  
55 and thus each is usually split into millions of small patches for processing.  
56 On the other hand, medical images are usually more difficult to analyze com-  
57 pared to generic images. The complex imaging parameters (contrast agents,  
58 machine settings), anatomic difference and interactions between different dis-  
59 eases result in a more complex analysis compared with natural images, where  
60 broad object categories are recognized and used for similarity calculations.  
61 The relevant changes of some medical images can be very subtle, which re-  
62 quire more fine-grained and detailed analysis. Therefore, directly employing  
63 traditional CBIR methods may not suitable for the large-scale medical image  
64 retrieval problem. In recent years, many efforts have been made to achieve  
65 large-scale medical image analytics, aiming to improve the efficiency and  
66 accuracy of image retrieval.

### 67 *1.1. Related Work*

68 There have been multiple reviews focusing on content-based medical im-  
69 age retrieval. The first review in the field was (Tang et al., 1999) but the  
70 text only contained few systems with a limited scope. Muller et al. (Müller  
71 et al., 2004) presented a first complete review that concentrates on image  
72 retrieval in the medical domain, where the techniques used in medical im-  
73 age retrieval, including visual feature extraction, image comparison, system  
74 evaluation, etc. are summarized. Subsequently, Long et al. (Long et al.,

75 2009) introduced four medical CBIR systems, i.e., CervigramFinder (Xue  
76 et al., 2008), SPIRS (Hsu et al., 2007), IRMA (IRMA), SPIRS-IRMA (An-  
77 tani et al., 2007). The authors also discussed future directions of medical  
78 image retrieval. Akgul et al. (Akgül et al., 2011) presented a comprehensive  
79 review about recent techniques of content-based image retrieval in radiol-  
80 ogy until 2011, including image features/descriptors, similarity measures and  
81 state-of-the-art systems. Additionally, they discussed challenges and future  
82 directions for the coming decade. Hwang et al. (Hwang et al., 2012) reviewed  
83 both text-based and content-based medical image retrieval systems, drawing  
84 a conclusion that the image retrieval service will be more effective if CBIR  
85 and semantic systems are combined. In 2013, Kumar et al. (Kumar et al.,  
86 2013) surveyed several applications and approaches to medical CBIR that  
87 focus on clinical imaging data that are multidimensional or acquired using  
88 multiple modalities such as combined PET-CT images.

89 Besides the abovementioned survey articles, the image retrieval task of  
90 the Conference and Labs of the Evaluation Forum, named ImageCLEF (Im-  
91 ageCLEF; Müller et al., 2010), has held several medical image retrieval tasks  
92 from 2004-2014. ImageCLEF provides a platform for research groups sub-  
93 mitting results and competing on the performance of their medical image  
94 retrieval methods. After each ImageCLEF medical image retrieval task, an  
95 overview is provided to summarize the methods and results of each compe-  
96 tition groups (de Herrera et al., 2013; Kalpathy-Cramer et al., 2015, 2011;  
97 Müller et al., 2012), which demonstrates the state-of-the-art in the medical  
98 image retrieval field. A benchmark for case-based retrieval including full vol-  
99 umetric images of more than 300 patients was run as part of the VISCERAL  
100 benchmark Jimenez-del-Toro et al. (2015).

### 101 1.2. Contributions and Organization of this Article

102 This survey provides a structured and extensive overview of large-scale  
103 retrieval for medical image analytics. Despite existing reviews having sum-  
104 marized varieties of medical retrieval systems and methods, none of them  
105 focused on the retrieval techniques for large-scale medical data, which is cur-  
106 rently the main challenge in the field of medical analytics. This survey offers  
107 a focused overview of the retrieval approaches for the large-scale medical im-  
108 age data by expanding multidisciplinary components that involve a nexus  
109 of the idea from machine learning, computer vision, information retrieval,  
110 and bioinformatics. It explains the entire process from scratch and presents  
111 a comprehensive pipeline that discusses every processing step from feature

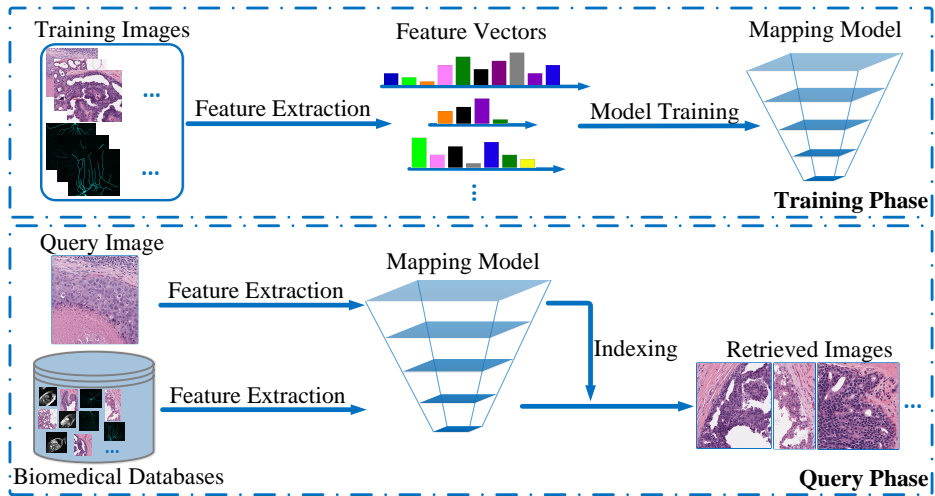


**Figure 1:** A general pipeline of large-scale medical image retrieval.

112 extraction to knowledge discovery and decision support. Fig. 1 illustrates a  
 113 general pipeline of large-scale medical image retrieval. Given a set of medi-  
 114 cal images (e.g., MRI, CT, microscopy, etc.), feature extraction methods are  
 115 employed to represent each image. Unlike traditional medical retrieval meth-  
 116 ods that directly compare the image similarity via original feature vectors,  
 117 large-scale approaches often first train a retrieval model, e.g., organizing and  
 118 transforming image features that can improve the performance of feature in-  
 119 dexing. In the query phase, the query image is compared only to similar  
 120 images based on the well-designed retrieval model rather than an exhaustive  
 121 search of the whole database. The retrieval results can be provided to users  
 122 for further analysis. According to Fig. 1, retrieval with large-scale medical  
 123 image databases is different compared with classical CBIR systems. In recent  
 124 years, many researchers in the medical domain have moved their attention to  
 125 the analytical questions of large-scale image analysis (Zhang and Metaxas,  
 126 2016). Therefore, in this era of big data, it is necessary to present a com-  
 127 prehensive review of recent advances in large-scale medical image analytics.

128  
 129 In this paper, we organize the survey into five parts: challenges/opportunities,  
 130 methodology review, evaluation protocols, applications, and future direc-  
 131 tions. In Section 2, challenges and opportunities related to big data in medi-  
 132 cal image analytics are provided. Section 3 and 4 discuss the methodology de-

133 tails relevant to the large-scale medical image retrieval, which mainly includes  
 134 two parts, i.e., feature representation, feature indexing and search. **Following**  
 135 **Section 5 introduces evaluation protocols in medical image retrieval.** Based  
 136 on the existing approaches, Section 6 reviews several applications of large-  
 137 scale medical image retrieval. Finally, Section 7 explores potential directions  
 138 for future work on large-scale medical retrieval.

## 139 2. Challenges and Opportunities

140 The challenges of large-scale medical image retrieval can be summarized  
 141 as a good trade-off between efficiency and accuracy. Despite traditional meth-  
 142 ods having already achieved good performance in many very specific medical  
 143 scenarios, keeping efficiency and accuracy in large-scale approaches still faces  
 144 many problems. Additionally, in the era of big data, large-scale medical im-  
 145 age analysis provides many opportunities for both academia and industry.

### 146 2.1. Challenges

147 One major concern in the big  
 148 data era is system efficiency. Given  
 149 the huge amount of medical image  
 150 data (WPS, 2010), how to repre-  
 151 sent and search in an efficient way  
 152 still has many challenges. Counting  
 153 the data from The Cancer Imaging  
 154 Archive (TCIA), a large-scale med-  
 155 ical image repository, Fig. 2 illus-  
 156 trates the number of images with the  
 157 six most common anatomical sites.  
 158 According to Fig. 2, these data sets  
 159 have hundreds of thousands to mil-  
 160 lions of medical images, which are  
 161 hard to analyze in real-time. For  
 162 medical image retrieval, each image  
 163 is usually represented by a feature  
 164 vector with often thousands of di-  
 165 mensions. An exhaustive search of millions of images with large feature  
 166 vectors is very time-consuming (Zhang et al., 2015c). In clinical applica-  
 167 tions, for a single patient tens to hundreds/thousands of images are collected

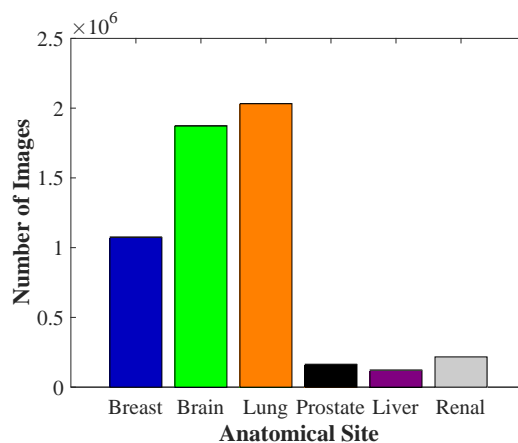


**Figure 2:** Number of medical images for the six most common anatomical area in the TCIA (The Cancer Imaging Archive) repository.

168 (large MRI studies can easily contains tens of thousand of single image slices  
 169 for a single patient) and an efficient retrieval of these images is required for  
 170 computer-assisted diagnosis. Accordingly, to achieve medical retrieval with  
 171 massive amounts of images, two aspects need to be explored for improvement  
 172 , i.e., 1) reducing the dimension of the feature vectors (or creating very sparse  
 173 spaces), 2) improving the strategy of similarity search or data indexing. Both  
 174 challenges are hard to tackle using conventional methods.

175 Another concern of medical retrieval is system accuracy. In the infor-  
 176 mation retrieval field, precision is one of the most important criteria for  
 177 performance evaluation, which is defined as the fraction of retrieved im-  
 178 ages that are relevant to the query image (Powers, 2011). For a query  
 179 image, higher retrieval precision indicates more reliable analysis and explo-  
 180 ration results, since most of the retrieved images share (hopefully) similar  
 181 semantic content with the query image. Retrieval precision plays a critical  
 182 role in medical analytics, where clinical diagnoses can depend on decision  
 183 support that is based on the retrieved images. However, achieving high  
 184 precision in medical retrieval is not an easy task, especially with the large  
 185 amount of volumetric image data, where most parts of the images/volumes  
 186 are not important for similarity calculations but small, local anomalies are.

187 Fig. 3 illustrates a common problem  
 188 in the classification of histopatho-  
 189 logical images, which are obtained  
 190 from intraductal breast lesions in  
 191 this case. The two images to the  
 192 left (with the blue bounding box)  
 193 belong to the same category, i.e.,  
 194 both are actionable (indicating the  
 195 cells/tumors are pathogenic). How-  
 196 ever, they have quite different ex-  
 197 pressions. On the other side, for  
 198 the bottom two images (with the  
 199 red bounding box), despite the vi-  
 200 sual similarity, they belong to dif-  
 201 ferent categories (the right image is  
 202 benign, indicating the cell's/tumor's  
 203 lack of the ability to invade neigh-  
 204 boring tissue and create metastasis).

205 This problem can be summarized as large intra-class variation and small

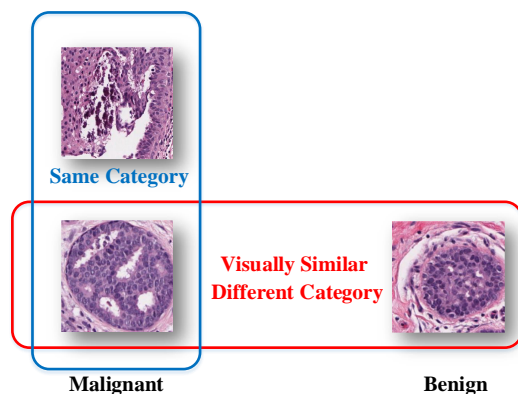


**Figure 3:** Three histopathology images of intraductal breast lesions. Classifying the breast histopathology images into benign or malignant is a challenge due to their large intra-class variation and small inter-class variation.

206 inter-class variation (Zhang et al., 2016b). Not only in histopathological im-  
207 age analysis, most medical image analytics tasks encounter similar problems.  
208 More critically, when dealing with massive medical data, this problem be-  
209 comes more challenging since more noisy images are included and influence  
210 the retrieval performance.

211 In addition to measuring efficiency and accuracy, the detailed evalua-  
212 tion protocol is also a challenging question in large-scale medical image re-  
213 trieval. Most of the traditional methods simply use class labels to evaluate  
214 the retrieval performance, which is not suitable for large-scale medical image  
215 databases, as they are most often not fully labeled and there can be different  
216 relevance expectations depending on the query images. Besides this, the data  
217 storage, access, organization, and computing techniques may also influence  
218 the retrieval performance of large-scale medical images. In this article, we  
219 review relevant methods and techniques that can tackle large-scale medical  
220 image retrieval.

## 221 2.2. Opportunities

222 Leaving aside the above challenges, large-scale image data brings unprece-  
223 dented opportunities to the medical field. In 2014, Siemens released a report  
224 saying that the market for medical imaging systems will grow from 32.3 bil-  
225 lion in 2014 to 49 billion in 2020 (Siemens). Without doubt, in the era of  
226 big data the development of large-scale medical analytics will accelerate this  
227 process. In a medical retrieval system, massive image data generally pro-  
228 vides more samples for similarity search, which can improve the accuracy  
229 and reliability of the system (Fang et al., 2016). More importantly, it also  
230 facilitates the research of knowledge discovery and pattern exploration in  
231 biomedical informatics. We illustrate two major opportunities that benefit  
232 from large-scale medical retrieval, i.e., computer-aided diagnosis and visual  
233 pattern exploration:

- 234 1. computer-aided diagnostics (CAD): CBIR methods have been proposed  
235 as an effective technology for CAD systems, which have the capacity  
236 of relieving the workload of doctors and to offer more reliable and con-  
237 sist analysis of medical images (Akgül et al., 2011; Depeursinge et al.,  
238 2011). Despite most retrieval systems are not routinely used, CBIR  
239 based CAD are rather research prototypes for medical image analytics.  
240 Given an image database with diagnosis information, CBIR methods  
241 aim to retrieve and visualize images with morphological profiles most



242 relevant to and consistent with the query image. This can provide deci-  
243 sion support, for example for pathologists (Kumar et al., 2013; Müller  
244 et al., 2004). When the CBIR-based CAD systems meet large-scale  
245 image databases, this benefit is enlarged by searching more relevant  
246 images with fine-grained content and morphologies. Retrieval results  
247 from large-scale databases can help pathologists to have accurate and  
248 deep understanding of query images, when they are unsure about spe-  
249 cific patterns.

- 250 2. visual pattern exploration: medical images contain a wealth of struc-  
251 tures and patterns that may convey information about underlying mech-  
252 anisms in biology (Peng et al., 2010; Schindelin et al., 2012). Generally,  
253 individuals with similar structures, shapes, morphologies will also ex-  
254 press similar functions and properties, such as neurons, tissue cells,  
255 etc. (Li et al., 2017a; Xing and Yang, 2016). By establishing large  
256 medical databases of visual data, CBIR systems can be used to iden-  
257 tify and explore unknown individuals based on the retrieval results.  
258 Massive image data are the basic requirement for such a medical ex-  
259 ploration. As individuals usually have complex shapes and varieties in  
260 the images, large-scale databases can provide more reliable results for  
261 pattern exploration, as it is more likely that similar patients exist of  
262 which images were taken with similar protocols.

263 Large-scale image databases bring new opportunities to innovate the tradi-  
264 tional medical retrieval systems, and some of the large-scale medical systems  
265 have already achieved good performance in clinical practice. In Section 6,  
266 we review relevant applications of large-scale medical retrieval.

### 267 3. Feature Representation

268 To achieve medical analytics from large-scale image databases, the first  
269 step is visual feature extraction, i.e., using feature vectors to represent each  
270 digital image. Generally, feature vectors are representing the low-level im-  
271 age content and can be linked to high-level perceptions of the images. A  
272 good feature representation is the prerequisite to achieve good performance  
273 in medical image retrieval. In recent years, a variety of feature representa-  
274 tions have been developed based on computer vision and machine learning.  
275 This section reviews recent advances in feature vectors in medical images.  
276 Specifically, the feature representation is classified into two categories, i.e.,

277 hand-crafted and learned features. This is mainly based on whether the fea-  
278 tures are obtained through domain expert knowledge (model-driven) or a  
279 purely data-driven procedures.

### 280 *3.1. Hand-crafted Features*

281 Generally, hand-crafted features are sequentially extracted from each im-  
282 age according to algorithms based generally on expert knowledge ([Antipov  
283 et al., 2015](#)), where each feature models a specific information such as color,  
284 texture or shape. Before the strong use of deep learning, hand-crafted meth-  
285 ods dominated the feature extraction field for several decades. Most current  
286 medical retrieval systems still employ hand-crafted methods for feature rep-  
287 resentation. In this subsection, we review typical hand-crafted features that  
288 have been used in medical image retrieval.

289 The most widely used hand-crafted features for image retrieval are based  
290 on the Scale-Invariant Feature Transform (SIFT) ([Lowe, 2004](#)). SIFT de-  
291 tects scale-invariant key points by finding local extrema in the difference-  
292 of-Gaussian (DoG) space. It describes each key point by a 128-dimensional  
293 gradient orientation histogram. Subsequently, all SIFT descriptors are mod-  
294 eled/quantized using a bag-of-words (BoW) ([Sivic and Zisserman, 2003](#)). The  
295 feature vector of each image is computed by counting the frequency of the  
296 generated visual words in the image. SIFT is a local texture feature that  
297 has achieved success in medical image retrieval (e.g., it was the most pop-  
298 ular feature in the ImageCLEF medical image retrieval task ([Müller et al.,  
299 2012](#))). Besides SIFT descriptors, many local descriptors can use the BoWs  
300 to generate local features for medical images, such as SURF (Speeded Up Ro-  
301 bust Features) ([Bay et al., 2008](#)), LBP (Local Binary Patterns) ([Ojala et al.,  
302 1996](#)) and others. In contrast to features extracted locally, holistic features  
303 are also widely adopted in medical image retrieval. These kinds of features  
304 can directly represent the global information of the entire image. For exam-  
305 ple, GIST ([Oliva and Torralba, 2001](#)) is a holistic feature which is based on  
306 a low dimensional representation of the scene that does not require any form  
307 of segmentation, and it includes a set of perceptual dimensions (naturalness,  
308 openness, roughness, expansion, ruggedness) that represent the dominant  
309 spatial structure of a scene ([Douze et al., 2009](#)). GIST has been applied in  
310 many medical image retrieval problems ([Kalpathy-Cramer and Hersh, 2008](#);  
311 [Liu et al., 2014a](#)). Other holistic features such as HOG (Histogram of Gaus-  
312 sians) ([Dalal and Triggs, 2005](#)), color histograms ([Siggelkow, 2002](#)) are also  
313 frequently used in medical image retrieval ([Müller and Deserno, 2010](#); [Yu](#)

Method	Category	Application
SIFT (Lowe, 2004)	Local, texture	Breast cancer (Zhang et al., 2015c), Basal-cell carcinoma (Wang et al., 2011a), etc
SURF (Bay et al., 2008)	Local, texture	Lung CTs (Haas et al., 2011), Body portion (Feulner et al., 2011), etc
LBP (Ojala et al., 1996)	Local, texture	2D-HeLa (Nanni et al., 2010), Brain MR (Murala et al., 2012), etc
GIST (Oliva and Torralba, 2001)	Holistic, shape	Mammogram (Liu et al., 2014a), Breast-tissue (Jiang et al., 2016a), etc.
HOG (Dalal and Triggs, 2005)	Holistic, texture	Cortical (Unay and Ekin, 2011), Lung (Song et al., 2012), etc
Color Histogram (Siggelkow, 2002)	Holistic, color	Organ (Caicedo et al., 2007), Dermatology (Bunte et al., 2011), etc.
Moments (Stricker and Orengo, 1995)	Holistic, shape	Multi-modalities (Rahman et al., 2007), Liver CT (Gletsos et al., 2003), etc.
Gabor filters (Manjunath and Ma, 1996)	Local, texture	Multi-modalities (Lim and Chevallet, 2005), Prostate Histopathology (Doyle et al., 2007), etc.
Tamura (Tamura et al., 1978)	Local, texture	Mammogram (Zhou et al., 2012), Multi-modalities (Güld et al., 2005), etc.
3D Riesz (Chenouard and Unser, 2011)	Local, texture	Epileptogenic Lesion (del Toro et al., 2013), 3D Multi-modalities (Jiménez-del Toro et al., 2015), etc

**Table 1:** Commonly used hand-crafted features and their applications in medical image retrieval.

314 et al., 2013). Table 1 lists some of the most commonly used hand-crafted  
315 features and their corresponding applications in medical image retrieval.

316 In addition to the common features mentioned above that can be used  
317 for the retrieval of both natural and medical images, there are many other  
318 hand-crafted features that are designed specifically for medical image data.  
319 In histopathology image analysis, the shape and texture information play an  
320 important role in the representation of cell/nuclei. Basavanahally et al. (Basa-  
321 vanhally et al., 2010) designed three graph-based features, i.e., Voronoi dia-  
322 gram, Delaunay triangulation, and minimum spanning tree, to describe the  
323 arrangement of the lymphocytes. Filipczuk (Filipczuk et al., 2013) employed  
324 25 kinds of features to represent cytological images, including the size of the  
325 nuclei, the texture features based on gray-level pixels, and the distribution of  
326 nuclei in the image. In general, these specific features are more discriminative  
327 than the general hand-crafted features. They achieved good performance in  
328 the detection, retrieval and analysis of cells and nuclei (Xing and Yang, 2016).  
329 Besides the histopathological images, specific features are also widely used  
330 for the representation of 3D medical image data, such as 3D brain tumors,  
331 neuronal morphology. For example, Cai et al. (Cai et al., 2010) developed  
332 PCM-based volumetric texture features for 3D neurological image retrieval,  
333 and Wan et al. (Wan et al., 2015) employed quantitative measurements and  
334 geometrical moments as features to represent the 3D neuron morphological  
335 data. Both achieved good performance in the retrieval task. A more general

336 system that creates many quantitative measurements of the brain including  
337 shape features is FreeSurfer (Fischl, 2012).

338 In order to achieve better retrieval performance, many researchers employ  
339 multiple hand-crafted features and combine them to represent each image.  
340 For example, Song et al. (Song et al., 2012) employed HOG and LBP features  
341 for retrieval and to recognize lung lesions. In general, combining multiple fea-  
342 tures (e.g., local and holistic features, common and specific features) obtains  
343 better performance compared with single feature systems (Lisin et al., 2005;  
344 Zhang et al., 2016a). Many groups in the ImageCLEF medical retrieval tasks  
345 have adopted this strategy (Simpson et al., 2012). However, when dealing  
346 with massive amounts of medical images, the combined features are often too  
347 large for scalable retrieval and may adversely affect the retrieval efficiency.  
348 Although a variety of features has been discussed above, for the medical re-  
349 trieval problem, there are no universal features that are suitable for all kinds  
350 of medical images. This is the case, as medical images are generated by  
351 different imaging techniques and tissues/organs usually have specific colors,  
352 textures and shapes. Even for the same tissue/organ, features may visu-  
353 ally differ under multiple dimensions and modalities (Kumar et al., 2013).  
354 Therefore, employing suitable hand-crafted features for a given kind of image  
355 data is an important and challenging step during medical retrieval. Feature  
356 selection can also be a step to create a subset of the features for a specific  
357 task.

358 Despite hand-crafted features having achieved many good results in medi-  
359 cal image retrieval, they have shortcomings when tackling large-scale medical  
360 data:

- 361 1. hand-crafted features need expert knowledge but expert knowledge usu-  
362 ally does not work well when the dataset is large as there may be out-  
363 liers and cases not covered by standardized rules;
- 364 2. feature extraction using hand-crafted methods is time-consuming and  
365 computationally expensive, especially when dealing with massive amounts  
366 of images;
- 367 3. many hand-crafted methods are only designed for specific medical data  
368 and can not be extended to other domains.

369 Accordingly, more automatic, efficient and extensible feature representation  
370 methods are required for the large-scale medical retrieval.

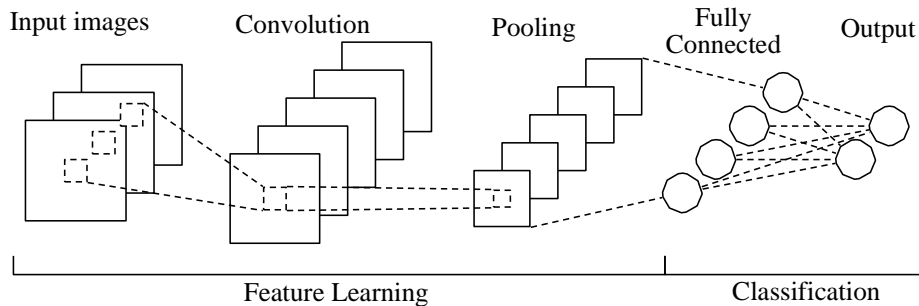


**Figure 4:** A general framework of convolutional neural networks.

371 *3.2. Learned Features*

372 In recent years, deep learning has become a hot topic and has achieved  
 373 very good results in feature representation, image classification, retrieval,  
 374 detection and other related fields. Compared with hand-crafted methods  
 375 using domain expert knowledge, deep learning requires only a set of train-  
 376 ing data that allows to discover the feature representations in a self-taught  
 377 manner (Bengio, 2009; LeCun et al., 2015). For the learned feature rep-  
 378 resentation, a variety of deep neural networks are designed nonlinearly and  
 379 hierarchically, i.e., mapping features from fine to abstract with multiple layers  
 380 of neural networks (e.g., tens to hundreds) and a large number of parameters  
 381 (e.g., thousands to millions) (Shen et al., 2016). In general, the prevalence  
 382 of deep learning mainly benefits from the availability of large training data  
 383 sets that make it possible to optimize the parameters. Accordingly, due to  
 384 the availability of current large-scale medical image databases, deep learning  
 385 can also be adopted to solve analytics tasks of medical images. Specifically,  
 386 both supervised and unsupervised deep neural networks have been explored  
 387 for creating feature representations of medical images.

388 Fig. 4 illustrates a general framework of a supervised deep neural net-  
 389 work, i.e., a Convolutional Neural Network (CNN) (LeCun et al., 1998).  
 390 The input images with fixed size are convolved with multiple learned ker-  
 391 nels using shared weights. Then, the pooling layers down-sample the input  
 392 representation nonlinearly and preserve the feature information in each sub-  
 393 region. Afterwards, the extracted features are weighted and combined in the  
 394 fully-connected layer, and these features are sent to a pre-defined classifier  
 395 for prediction. Finally, by comparing the output class with the image label,  
 396 the CNN parameters (e.g., kernels, weights, bias) are updated in each iter-

397 ation. Recent results, as on the ImageNet Large Scale Visual Recognition  
398 Challenge (ILSVRC) (Russakovsky et al., 2015) have shown the excellent  
399 performance of very deep neural networks, where more convolution, pooling  
400 and fully connected layers are employed than before, and more complicated  
401 network structures are developed, e.g., AlexNet (Krizhevsky et al., 2012),  
402 GoogLeNet (Szegedy et al., 2015), VGG Net (Simonyan and Zisserman, 2014)  
403 and ResNets (He et al., 2015).

404 Supervised deep neural networks require a large amount of labeled im-  
405 ages to train the parameters in each layer. However, in the medical field,  
406 the amount of labeled images is typically limited. Simply training deep  
407 neural networks from scratch using small-sized labeled data can easily re-  
408 sult in overfitting (Srivastava et al., 2014). Thus, researchers have proposed  
409 several methods to accommodate medical image analysis with deep neural  
410 networks. For example, Bar et al. (Bar et al., 2015) learned features for chest  
411 pathology detection using a Decaf pre-trained CNN model (Donahue et al.,  
412 2014), and the parameters are trained from non-medical datasets such as Im-  
413 ageNet (Deng et al., 2009). In ImageCLEFmed 2016, NovaSearch adopted  
414 CNN models that are trained from scratch using only the provided medi-  
415 cal data (Semedo and Magalhães). They employed several techniques (e.g.,  
416 Dropout (Srivastava et al., 2014), data augmentation) to deal with the un-  
417 balanced and small data sets. According to (Shin et al., 2016), there are  
418 three major techniques that can successfully learn feature representation of  
419 medical images through CNNs:

- 420 1. pre-training the CNN model on natural images and fine-tuning on med-  
421 ical target images; this technique has been used for lung images (Hof-  
422 manninger and Langs, 2015; Li et al., 2014a; Schlegl et al., 2014), brain  
423 MRI (Li et al., 2014b), etc.;
- 424 2. training the CNN model from scratch using only medical images, and  
425 employing several measures to avoid overfitting; this technique has been  
426 used in cardiac CT (Wolterink et al., 2015), on lung nodules (Shen  
427 et al., 2015d), etc.;
- 428 3. using a pre-trained CNN model to extract features, employing these  
429 features as complementary information and combining them with hand-  
430 crafted features; these combined features have been used on chest X-  
431 rays (Bar et al., 2015), pulmonary peri-fissural nodules (Ciompi et al.,  
432 2015), etc.

433 Although supervised deep neural networks have demonstrated excellent per-

434 performance in feature representation, they require a large amount of manually  
 435 labeled training data. However, unlike the annotation of natural images that  
 436 is easy to achieve, the labels of many medical images can only be annotated  
 437 by physicians or domain experts, which is expensive. In many cases, the  
 438 ground truth labels are simply unavailable, as the exact patterns of some  
 439 abnormalities are still unidentified or very subjective in nature (e.g., neuron  
 440 images, precise tumor regions). To overcome the limitations of supervised  
 441 feature learning, multiple unsupervised deep neural networks have been pro-  
 442 posed for feature representation (Bengio et al., 2012). Fig. 5 illustrates a  
 443 typical unsupervised neural network, i.e. an Auto-Encoder (Bourlard and  
 444 Kamp, 1988). Given the input images  $\mathbf{X}_m$ , it learns the feature represen-  
 445 tations  $h^{(2)}$  by minimizing the reconstruction error between the input and  
 446 the output, i.e.,  $\mathbf{Y}_m \approx \mathbf{X}_m$ , which indicates the decoder results should ap-  
 447 proximate the input. Despite the single layer auto-encoder being too shallow  
 448 to learn features, the representation power improves significantly when sev-  
 449 eral auto-encoders are stacked to form deep stacked auto-encoders (SAEs).  
 450 For example, Wu et al. (Wu et al., 2013, 2016) developed an unsupervised  
 451 feature selection method using a convolutional stacked auto-encoder to iden-  
 452 tify intrinsic deep feature representations in image patches. The method  
 453 is demonstrated on 7.0-tesla brain MR images, validating that unsupervised  
 454 feature learning is effective for brain MR registration. Besides this, Shin (Shin  
 455 et al., 2013) employed stacked auto-encoders for unsupervised feature learn-  
 456 ing and organ identification in magnetic resonance images, where visual and  
 457 temporal hierarchical features are learned to categorize object classes from  
 458 an unlabeled multimodal DCE-MRI data set (Collins and Padhani, 2004).

459 In addition to auto-encoders,  
 460 restricted Boltzmann machines (RBM) (Smolens-  
 461 sky, 1986) can also construct un-  
 462 supervised deep neural networks,  
 463 e.g. deep belief networks (Hinton  
 464 and Salakhutdinov, 2006) and deep  
 465 Boltzmann machines (Salakhutdi-  
 466 nov, 2015). These deep neural net-  
 467 works are also the common choice  
 468 to tackle medical feature represen-  
 469 tations and other medical analyt-  
 470 ics tasks. For example, Brosch and  
 471 Tam (Brosch et al., 2013) performed

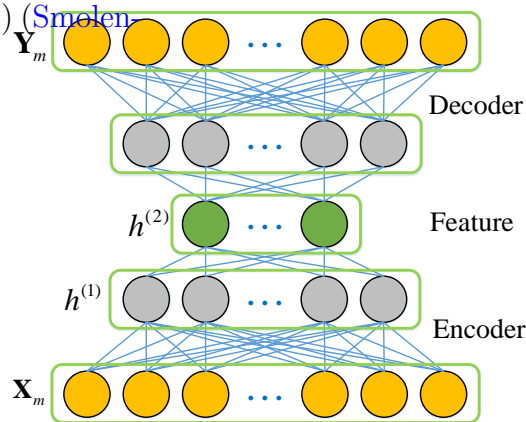


**Figure 5:** The hierarchical structure of an auto-encoder.

472 manifold learning by reducing the  
473 dimensionality of brain images using  
474 a deep belief network that can dis-  
475 cover patterns of similarity in groups of images. Cao et al. (Cao et al., 2014)  
476 developed a multimodal approach for medical image retrieval that is based on  
477 deep Boltzmann machines. Experimental results demonstrate that the new  
478 deep Boltzmann machine-based multimodal learning model is a promising  
479 solution for next-generation medical image indexing and retrieval systems.

480 For large-scale medical image analytics, learned feature representations  
481 are a clear trend, since more and more images are available to train the  
482 deep neural networks. However, the usage of deep learning for medical im-  
483 age retrieval is not frequent. One reason is that previously most medical  
484 image retrieval tasks only had to tackle small-sized data sets (e.g., hundreds  
485 to thousands of images at the most), which does not allow the training of  
486 deep neural networks. The other reason is that for some specific medical im-  
487 ages the hand-crafted features designed by domain experts can achieve very  
488 good performance when the data sets are not too large (e.g., the holistic  
489 features of histopathological images (Basavanhally et al., 2010)). Due to the  
490 multi-modality, complexity (e.g., diverse medical imaging techniques, com-  
491 plex structures and morphology of tissues/organs) and also quickly changing  
492 image acquisition devices, the specified hand-crafted features are still useful  
493 in many medical image retrieval scenarios. Additionally, the deep-learning  
494 based methods are capable to learn different types of features compared with  
495 hand-crafted methods. Thus the learned features also play a critical role  
496 in the feature representation of medical images, particularly when the data  
497 sets are large. In the ImageCLEF Challenges (García Seco de Herrera et al.,  
498 2016), many groups employed both learned features and hand-crafted fea-  
499 tures to represent medical images. Then, these features are fused for more  
500 accurate retrieval and classification results.

#### 501 4. Feature Indexing and Search

502 After feature extraction, each image is represented by a feature vec-  
503 tor. The medical image retrieval problem can now be treated as a nearest-  
504 neighbor search among these feature vectors, i.e., computing and ranking  
505 the distance between the query image(s) or volume(s) and all images in the  
506 databases. However, when handling large-scale databases, exhaustive search  
507 among long feature vectors is time-consuming. Sequentially computing the



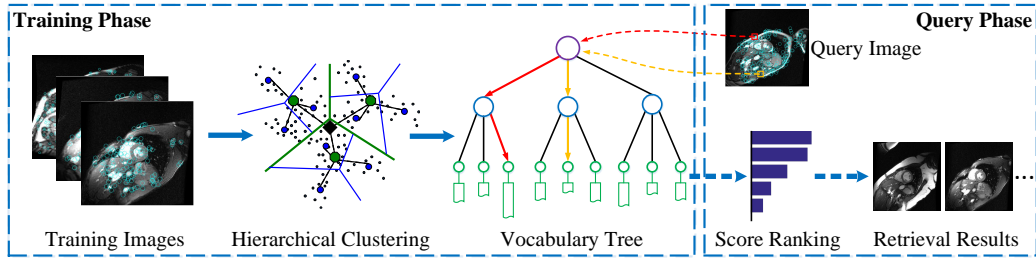


**Figure 6:** A framework for vocabulary tree based image retrieval.

508 distance of millions of high-dimensional feature vectors is unfeasible. In this  
 509 section, we review recent advances that can efficiently and accurately tackle  
 510 feature indexing in large-scale medical retrieval.

#### 511 4.1. Vocabulary Tree

512 The vocabulary tree was first proposed by Nistér and Stewénius (Nister  
 513 and Stewenius, 2006). It is widely used for scalable image retrieval (Wang  
 514 et al., 2011b; Zhang et al., 2015b). It builds a tree-structure to accelerate  
 515 similarity indexing. Compared with traditional methods based on exhaus-  
 516 tive search of image features, vocabulary tree based methods employ a hi-  
 517 erarchical tree and inverted files that can significantly improve the retrieval  
 518 efficiency. Fig. 6 presents the framework of vocabulary tree based image  
 519 retrieval. The framework can be divided into two phases, i.e., the training  
 520 phase (offline) and the query phase (online). The training phase builds the  
 521 indexing model (hierarchical tree-structure) from given image sets and the  
 522 query phase returns images that are similar to the query image.

523 **Training Phase:** For a set of training data, vocabulary tree methods  
 524 first detect key points in each image (denoted as the cyan circles in Fig. 6).  
 525 The key points can be defined as corners with scale and rotation invariance,  
 526 as well as interest points specified by domain experts. Subsequently, these  
 527 key points are represented by local feature vectors (e.g., SIFT (Lowe, 2004)),  
 528 and the descriptors from all training images are collected for hierarchical  $k$ -  
 529 means clustering. Specifically, instead of defining  $k$  as the final number of  
 530 clusters,  $k$  is defined as the number of children centers in each cluster. After  
 531  $L$  recursive clustering, a tree-structure of depth  $L$  and branch factor  $k$  is  
 532 built, where each tree node (also referred to as the visual word) corresponds  
 533 to a cluster center. Each leaf node includes several key points that are close

534 to each other visually. Accordingly, all images in the database are added to  
535 inverted files attached to the leaf nodes with respect to their corresponding  
536 key points. Afterwards, the vocabulary tree-structure and the inverted file  
537 are used for the indexing of the images.

538 **Query Phase:** Given a query image  $q$ , its key points are extracted and  
539 set as the input in the vocabulary tree. By comparing with nodes in each hi-  
540 erarchy, each key point can reach a leaf node attached to an inverted file. As  
541 each inverted file records images relevant to the leaf node, the similarity scores  
542 can be computed between  $q$  and the images in corresponding inverted files.  
543 Normally, the term frequency-inverse document frequency (TF-IDF) (Salton  
544 and Buckley, 1988) is adopted as the similarity score to balance the im-  
545 portance of a visual word to an image in a collection. By ranking all the  
546 similarity scores in descending order, the top ranked images can be consid-  
547 ered as the retrieval results. Unlike previous methods simply comparing the  
548 similarity of all the key points between two images, vocabulary tree methods  
549 construct the hierarchical tree-structure and index similar images using the  
550 inverted files. For each key point vector, only a total of  $kL$  dot products  
551 are needed, which is very efficient if  $k$  is not large. More importantly, the  
552 inverted file strategy can significantly improve the indexing process since it  
553 does not need to traverse the whole image database.

554 Vocabulary trees and its variants have been applied for large-scale med-  
555 ical image retrieval. They do not only improve the computational efficiency  
556 but are also often more accurate compared with traditional retrieval methods.  
557 For example, Jiang et al. (Jiang et al., 2015a,c) proposed an adaptive weight-  
558 ing strategy in the vocabulary tree based framework to tackle mammogram  
559 image retrieval. As the features with high frequencies in a mammogram are  
560 less informative than those with low frequencies, to avoid overcounting, they  
561 incorporate mammogram-specific node frequencies into the IDF scheme to  
562 down-weight the high-frequency features. The adaptive weighting technique  
563 is very effective to retrieve these specific images, i.e., mammographic masses.  
564 Wang et al. (Wang et al., 2015) designed a discriminative and generative  
565 vocabulary tree for the authentication and recognition of finger vein images.  
566 This method considers both the discriminative appearance of local image  
567 patches and their generative spatial layout. The training process remains the  
568 same as building a conventional vocabulary tree, while the prediction process  
569 uses a proposed point set matching method to support non-parametric patch  
570 layout matching. This joint discriminative and generative model can achieve  
571 good performance in finger vein images, since the employed vocabulary tree

572 model can retain the efficiency for the whole system. More importantly, the  
573 point set matching strategy considers the geometrical layout of local image  
574 patches, which is more accurate compared with previous vocabulary tree  
575 based methods that only consider the description of local key points.

576 By changing the similarity indexing strategy, vocabulary tree based meth-  
577 ods have achieved efficient retrieval in large-scale databases. As these kinds  
578 of methods directly employ local feature descriptors instead of the global  
579 features, it can be applied to most medical images, including both 2D and  
580 3D images where local key points can be detected and described. However,  
581 vocabulary tree based methods also have several limitations. For example,  
582 simply using local features is not enough to represent and discriminate some  
583 specific medical types of images, e.g., for some lung images, the global shape  
584 should be considered during retrieval. In addition, the training phase in  
585 building the hierarchical vocabulary tree is usually time-consuming, espe-  
586 cially when tackling very large image databases (search on a database with  
587 millions of images). In practical applications, to achieve good results, vo-  
588 cabulary tree based methods also rely heavily on parameter tuning, i.e., the  
589 number of each cluster center  $k$ , total levels of the hierarchical tree  $L$ . Thus,  
590 more efficient and accurate methods need to be developed for large-scale  
591 medical image retrieval.

## 592 4.2. Hashing

593 In recent years, hashing methods have been intensively investigated in  
594 the machine learning and computer vision fields for indexing big data ([Wang  
595 et al., 2016](#)). Instead of directly searching nearest neighbors from an original  
596 data set, hashing methods first compress the original data into short binary  
597 codes (e.g., tens to hundreds of bits) based on the defined hashing functions.  
598 Then, the nearest-neighbor search is more efficient by computing the similar-  
599 ity distances in binary Hamming space rather than in the high-dimensional  
600 feature space.

### 601 4.2.1. Hashing Frameworks

Fig. 7 presents the framework of hashing-based image retrieval. Assum-  
ing we have  $n$  medical images in the database, after feature representa-  
tion these  $n$  images are represented by  $d$  dimensional feature vectors, i.e.,  
 $\mathbf{X} = \{\mathbf{x}_1, \mathbf{x}_2, \dots, \mathbf{x}_n\} \subset \mathbb{R}^{d \times n}$  (denoted as the blue points in Fig. 7). For the  
image  $\mathbf{x}_i \subset \mathbb{R}^{d \times 1}$ , its feature space can be split by a set of hashing functions  
 $H = \{h_1, h_2, \dots, h_K\} \subset \mathbb{R}^{d \times K}$ , and each hashing function encodes  $\mathbf{x}_i$  into one

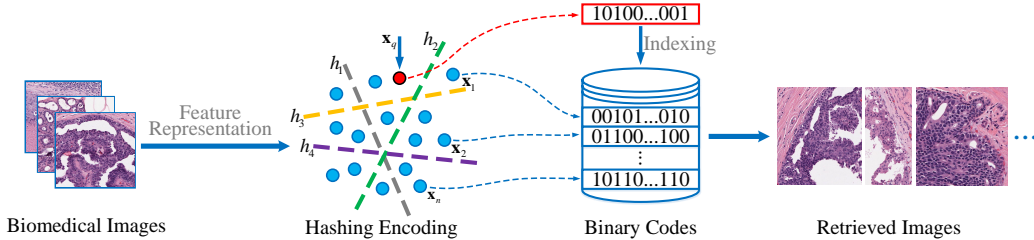


**Figure 7:** The framework of hashing-based image retrieval.

bit of binary code  $h_k(\mathbf{x}_i)$ . Therefore, the corresponding  $K$  bits of binary code of  $\mathbf{x}_i$  can be denoted as:

$$\mathbf{y}_i = H(\mathbf{x}_i) = \{h_1(\mathbf{x}_i), h_2(\mathbf{x}_i), \dots, h_K(\mathbf{x}_i)\} \quad (1)$$

In practice, for computational convenience, the above hashing functions are usually substituted by the projected matrix  $\mathbf{w} \in \mathbb{R}^{d \times K}$  and the intercept vector  $\mathbf{b} \in \mathbb{R}^{K \times 1}$ :

$$\mathbf{y}_i = \text{sgn}(f(\mathbf{w}^T \mathbf{x}_i + \mathbf{b})) \quad (2)$$

602 where  $f(\cdot)$  is a pre-specified function that can be linear or nonlinear. Then,  
 603 all images in the database are represented by the mapped binary codes. The  
 604 query image  $\mathbf{x}_q$  (denoted as the red point in Fig. 7) can also be mapped into  
 605 binary codes through Eq. 2. Subsequently, the similarity search between  
 606 the query and each image in the database is transformed as the Hamming  
 607 distance ranking of their corresponding binary codes, which is very fast. The  
 608 key question of hashing methods is how to obtain good hashing functions  
 609 that can not only split the feature space via binary encoding but also keep  
 610 similarities and diversity among the original data.

#### 611 4.2.2. Categories of Hashing Methods

612 The methods to compute hashing functions can be roughly divided into  
 613 two categories, i.e., data-independent and data-dependent. Data-independent  
 614 methods usually design generalized hashing functions that can compact any  
 615 given data set into binary codes. Locality-Sensitive Hashing (LSH) and its  
 616 variants are the most popular data-independent methods (Gionis et al., 1999;  
 617 Kulis et al., 2009; Raginsky and Lazebnik, 2009). LSH-based methods com-  
 618 pute hashing functions via maximizing the probability of collision for similar

619 items, which can keep the originally nearby data points mapping into the  
620 same bit with high probability. However, this type of method often needs  
621 long binary codes and many hashing functions to ensure the desired retrieval  
622 precision, which dramatically increases the storage costs and the query time.  
623 More importantly, as these hashing functions are designed independently  
624 from the training data sets, it is hard to ensure the retrieval performance for  
625 any given data set.

626 Another category are the data-dependent methods (also called learning to  
627 hash methods) that learn the hashing functions from a given training data set.  
628 In general, compared with data-independent methods, data-dependent meth-  
629 ods can achieve comparable or even better retrieval accuracy with shorter  
630 binary codes. Currently, many learning-based hashing methods have been  
631 applied for large-scale medical image retrieval, including but not limited to,  
632 Iterative Quantization (ITQ) (Gong et al., 2013), Kernel-Based Supervised  
633 Hashing (KSH) (Liu et al., 2012), Anchor Graph Hashing (AGH) (Liu et al.,  
634 2011), Asymmetric Inner-product Binary Coding (AIBC) (Shen et al., 2015a)  
635 and others. Accordingly, the taxonomy of data-dependent hashing methods  
636 can be defined in multiple viewpoints. For example, based on whether the  
637 training data sets have labels or not, hashing methods can be divided into  
638 supervised, unsupervised and semi-supervised methods. Supervised methods  
639 employ advanced machine learning techniques such as kernel learning, metric  
640 learning, and deep learning to compute the hashing functions from labeled  
641 training data. Many supervised hashing methods have achieved good per-  
642 formance since they can shorten the semantic gap between the compacted  
643 binary codes and the image labels (Fan, 2013; Gordo et al., 2014; Norouzi  
644 et al., 2012; Shen et al., 2015b). Without label information, unsupervised  
645 methods explore the properties of training data sets such as distributions  
646 and manifold structures to design effective hashing functions. Representa-  
647 tive methods include spectral hashing (Weiss et al., 2009), graph hashing (Liu  
648 et al., 2014b), manifold hashing (Shen et al., 2013), etc. Additionally, semi-  
649 supervised methods design hashing functions using both labeled and unlabeled  
650 data. These kinds of methods can improve the binary encoding per-  
651 formance by leveraging semantic similarity with limited image labels while  
652 remaining robust to overfitting (Jain et al., 2009, 2008; Wang et al., 2012).  
653 Another taxonomy of data-dependent methods is based on the form of the  
654 hashing functions, i.e., linear and nonlinear. Linear hashing functions sep-  
655 arate and map the original feature space with simple projections (as shown  
656 in Fig. 7,  $\{h_1, h_2, \dots, h_K\}$ ). They are computationally efficient and easy to

Method	Taxonomy	Application
PCA Hashing (Gong and Lazebnik, 2011; Yu et al., 2013)	Unsupervised Linear	Multi-modality images (Yu et al., 2013)
Kernelized Hashing (Liu et al., 2012)	Supervised Nonlinear	Brest histopathology (Zhang et al., 2015c) Cell-level histopathology (Zhang et al., 2015d)
Composite Hashing (Gong et al., 2013; Liu et al., 2011)	Unsupervised Nonlinear	Digital mammogram (Liu et al., 2016b)
Hashing Forest (Conjeti et al., 2016a)	Unsupervised Linear	Neuron morphology (Mesbah et al., 2015; Yu and Yuan, 2014)
MIPS Binary Coding (Shen et al., 2015a)	Unsupervised Nonlinear	Neuron morphology (Li et al., 2017a)
Deep Autoencoder (Sze-To et al., 2016; Vincent et al., 2010)	Unsupervised Nonlinear	X-ray images (Sze-To et al., 2016)

**Table 2:** Existing hashing based large-scale medical image retrieval methods with their taxonomies and applications

657 optimize (Gong et al., 2012; He et al., 2012; Trzcinski and Lepetit, 2012).  
658 However, linear hashing functions can not handle the situation when the  
659 difference among image data are subtle and linearly inseparable. Thus, non-  
660 linear hashing was developed to override such limitations. Such methods  
661 learn hashing functions based on kernel matrixes or manifold structures and  
662 can embed the intrinsic structure in a high-dimensional space and nonlin-  
663 early map feature vectors into binary codes (Kulis and Grauman, 2012; Liu  
664 et al., 2012; Shen et al., 2015c).

#### 665 4.2.3. Methodology Review

666 Table. 2 summarizes the existing hashing-based medical retrieval meth-  
667 ods, as well as their corresponding taxonomies and applications. According  
668 to Table. 2, both supervised and unsupervised, linear and nonlinear hashing  
669 methods have been developed for medical retrieval. In this subsection, we  
670 briefly review the above hashing methods and also discuss their advantages  
671 and drawbacks.

672 **PCA Hashing** (Yu et al., 2013): it first linearly projects raw image fea-  
673 tures into uncorrelated dimensions via Principal Component Analysis (PCA),  
674 where each new feature dimension is orthogonal to each other. Then, it learns  
675 the hashing function (i.e. a rotation matrix) by minimizing the binarization  
676 error between the new feature matrix and the corresponding binarized fea-  
677 ture matrix (Gong and Lazebnik, 2011). PCA Hashing demonstrates high  
678 computational efficiency and comparable retrieval precision compared with  
679 traditional feature-based nearest-neighbor search. However, since both PCA  
680 projection and hashing function optimization are linear, PCA hashing can-

681 not achieve good performance when tackling medical images that are complex  
682 (e.g., image differences are subtle, the feature space is not linearly separable).

683 **Kernelized Hashing** (Zhang et al., 2015c): for most medical images,  
684 linear inseparability is a critical constraint that needs to be taken into account  
685 during large-scale retrieval. To tackle this challenge, Kernelized Hashing con-  
686 sideres the hashing function with kernels, since kernel methods can map the  
687 feature vectors into a high-dimensional space and make the linearly insepara-  
688 ble images easy to differentiate. Accordingly, the learned binary codes from  
689 kernelized hashing are also able to differentiate complex medical images. In  
690 addition, Kernelized Hashing designs a supervised framework by collaborat-  
691 ing kernel functions with medical labels (e.g., labeling the histopathological  
692 image with benign or malignant). The supervised information significantly  
693 boosts the retrieval performance since it can bridge the semantic gap between  
694 low-level features and high-level clinical analytics.

695 **Composite Hashing** (Liu et al., 2016b): this algorithm can generate  
696 more effective hash codes by integrating global features (e.g. GIST (Oliva and  
697 Torralba, 2001)) and local features (e.g. SIFT (Lowe, 2004)) with different  
698 distance metrics. In general, single types of features can not comprehensively  
699 represent a medical image. On the other side, simply combining multiple  
700 features may also fail to achieve accurate image retrieval, since each type  
701 of feature has its specific meaning and representation. Thus, Composite  
702 Hashing improves the Anchor Graph with multiple features and fuses them  
703 by distance metric and local manifold. Then, it learns the hashing function  
704 using iterative quantization.

705 **Hashing Forests** (Conjeti et al., 2016a): this approach learns binary  
706 codes by training independent hashing trees. For the internal node in each  
707 tree, locality preserving projections are employed to project data into a la-  
708 tent subspace, where separability between dissimilar points is enhanced. For  
709 each input image, each trained tree generates several bits of binary codes,  
710 and the combination of these binary codes in the forest is used to represent  
711 the input image. Additionally, it employs an inverse-lookup search scheme  
712 to improve the efficiency of similarity comparisons. Hashing Forests can  
713 generate any given length of binary codes, which is particularly suitable for  
714 low-dimensional image features.

715 **MIPS Binary Coding** (Li et al., 2017a): as demonstrated in (Liu et al.,  
716 2012; Shen et al., 2015a), the Hamming distance and the inner code product  
717 have a one-to-one correspondence. Thus, unlike the above methods based  
718 on the Hamming distance metric, MIPS (Maximum Inner Product Search)

719 Binary Coding introduces a new objective based on the inner code product,  
720 which is more likely to learn non-linear hashing functions. Specifically, by  
721 adopting an alternative iteration strategy, it learns two asymmetric hashing  
722 functions for the image database and the query image respectively. This  
723 strategy can make the inner product based objective easy to optimize. It also  
724 promotes the hashing functions to map binary codes into a high-dimensional  
725 non-linear space.

726 **Deep Autoencoders** (Sze-To et al., 2016): this algorithm employs deep  
727 architectures to hash medical images into binary codes without class labels.  
728 Specifically, it uses a specific unsupervised deep architecture, namely deep de-  
729 noising autoencoders (DDA) (Vincent et al., 2010) to enhance feature learn-  
730 ing and binary coding with four steps: image pre-processing, unsupervised  
731 layer-by-layer training, unsupervised fine-tuning with dropout, and decoder  
732 removal. Finally, a threshold ( $> 0.5$ ) is applied on the real-valued feature  
733 vectors to obtain binary codes. Deep Autoencoders learn binary codes with-  
734 out using any supervised information, which is suitable for medical images  
735 where labels are hard to obtain.

736 When using hashing methods to tackle large-scale medical image retrieval  
737 problems, we should not only focus on the hashing methods itself but also  
738 need to consider their possible adaptations for different medical image data  
739 sets. When the annotation of all medical images in data sets are available, su-  
740 pervised hashing methods are more suitable and are generally more accurate  
741 than unsupervised and semi-supervised hashing. For example, Kernel-Based  
742 Supervised Hashing (KSH) (Liu et al., 2012), Supervised Discrete Hashing  
743 (SDH) (Shen et al., 2015b), Deep Supervised Hashing (DSH) (Liu et al.,  
744 2016a) can achieve excellent performance in many public data sets. However,  
745 in many cases when the medical image annotations are not easy to acquire,  
746 semi-supervised/unsupervised hashing is a more reasonable choice (e.g., Dis-  
747 crete Graph Hashing (DGH) (Liu et al., 2014b), MIPS (Shen et al., 2015a),  
748 Semi-Supervised Hashing (SSH) (Wang et al., 2012)). In addition, for some  
749 medical images that are not easy to differentiate, non-linear hashing meth-  
750 ods can usually achieve much better retrieval performance, such as Inductive  
751 Manifold-Hashing (IMH) (Shen et al., 2013), AGH (Liu et al., 2011), de-  
752 spite training non-linear hashing functions being more time-consuming than  
753 training linear hashing functions.



754 *4.3. Other Methods*

755 Besides the vocabulary tree and hashing, there are many other methods  
756 that have been designed to tackle the feature indexing of large-scale medical  
757 image databases. These methods can be either accelerating the similarity  
758 search or improving the retrieval accuracy. We briefly introduce and discuss  
759 these methods.

760 *4.3.1. Feature Compression*

761 Indexing in large medical databases is usually very time-consuming, es-  
762 pecially when the images are represented by high dimensional features. To  
763 accelerate the indexing process, one kind of methods is feature compression,  
764 which can compress long image features into a smaller size. Hashing belongs  
765 to the category of feature compression that is discussed above. In addition to  
766 hashing, many other compression methods have been employed for efficient  
767 medical image retrieval.

768 Principal components analysis (PCA) is one of the most popular method  
769 for feature compression. After feature extraction, medical images can be  
770 represented by single or multiple feature vectors that have high dimension.  
771 Many medical image retrieval methods have employed PCA to reduce the  
772 feature dimensionality. For example, Tian et al. (Tian et al., 2008) first pre-  
773 sented a global and local texture feature combination for the description of  
774 medical images. Then, they adopted PCA to reduce the dimension of the  
775 combined features. In the analytics of histopathological images, Sertel et  
776 al. (Sertel et al., 2009) introduced a novel color-texture analysis approach  
777 that combines a model-based intermediate representation with low level tex-  
778 ture features. Then, PCA and LDA (linear discriminant analysis (Fukunaga,  
779 2013)) are employed for feature dimensionality reduction. PCA-based med-  
780 ical image retrieval can significantly reduce the feature dimensionality and  
781 usually demonstrates comparable performance with the methods using the  
782 original features.

783 In addition to PCA, multiple methods have been proposed for medical  
784 feature compression in recent years. In (Foncubierto-Rodríguez et al., 2013),  
785 Foncubierto-Rodríguez et al. presented a medical image retrieval method us-  
786 ing a bag of meaningful visual words. As visual vocabularies are often redun-  
787 dant, over-complete and noisy, they presented a pruning technique based on  
788 probabilistic latent semantic analysis (PLSA) (Hofmann, 2001). The PLAS  
789 pruning can enormously reduce the feature dimension when describing a med-  
790 ical image data set with no significant effect on accuracy. More recently, Lan

791 and Zhou (Lan and Zhou, 2016) proposed a simple yet discriminant feature,  
792 called histogram of compressed scattering coefficients (HCSCs) for medical  
793 image retrieval. They first performed a particular variation of deep convo-  
794 lutional networks, i.e., the scattering transform, to yield high dimensional  
795 features. Then a compression operation is carried out on the obtained coef-  
796 ficients for a dimensionality reduction.

#### 797 4.3.2. Re-ranking

798 After the similarity indexing through feature compression and other large-  
799 scale methods, a set of top ranked medical images can be efficiently computed  
800 based on a distance measure. However, these retrieved images may not always  
801 correspond to what a human would want and the retrieval precision can vary  
802 strongly using different features. Therefore, re-ranking of the coarse results  
803 is expected to further improve the retrieval performance for more accurate  
804 retrieval. Particularly, re-ranking methods can reorder the initially retrieved  
805 images to move the most relevant images to the top or optimise diversity in  
806 the top results.

807 In recent years, multiple methods have been proposed for re-ranking in  
808 different image retrieval applications. In the medical domain, based on the  
809 information employed for re-ranking, the re-ranking methods can be roughly  
810 divided into three categories, i.e., textual-visual based, multi-feature based  
811 and user-feedback based. In the following, we briefly review relevant articles  
812 about the three categories respectively:

- 813 1. Textual-visual based: these kinds of methods first retrieve relevant  
814 medical images through textual indexing, then the initial results are  
815 re-ranked by considering the visual similarity. Textual-visual based re-  
816 ranking was adopted by many groups in the ImageCLEF medical image  
817 retrieval tasks. For example, Radhouani et al. (Radhouani et al., 2009)  
818 introduced their work at ImageCLEF 2009. They first leveraged textual  
819 data to search relevant images in three domain dimensions, anatomy,  
820 pathology and modality. Then, they employ the visual data to re-  
821 rank the document lists based on the extracted features, including a  
822 color and intensity histogram, gray-level co-occurrence matrices and  
823 other features. Besides this, Depeursinge and Müller (Depeursinge and  
824 Müller, 2010) described several fusion techniques for combining textual  
825 and visual information that were used in ImageCLEF.
- 826 2. Multi-feature based: this kind of method first computes the retrieval  
827 results from multiple kinds of features, then the final results are ob-

828 tained by fusing and re-ranking the above retrieved images. Recently,  
829 Zhang et al. (Zhang et al., 2016a) presented a method for histopathol-  
830 ogy image analysis by re-ranking the results from multiple features.  
831 Specifically, after obtaining several top ranked relevant images from  
832 multiple kinds of features, they employed a graph-based query-specific  
833 fusion approach where multiple retrieval results are integrated and re-  
834 ordered based on a fused graph (Zhang et al., 2015b). In general, such  
835 re-ranking methods can significantly improve the retrieval performance  
836 since they consider the image similarity and discrimination from several  
837 viewpoints using multiple features, e.g., local and holistic features.

- 838 3. User-feedback based: after receiving the initial results, this kind of  
839 method re-ranks the retrieved images based on relevance feedback from  
840 users. The relevance feedback can specify which image is relevant/irrelevant.  
841 Agarwal and Mostafa (Agarwal and Mostafa, 2011) employed the user-  
842 feedback based re-ranking for the Alzheimer’s disease detection. They  
843 first described a content-based image retrieval system, i.e., ViewFinder  
844 Medicine (vfM), to combine visual and textual features for initial in-  
845 dexing. Then the retrieval system employed the user-provided feed-  
846 back to perform re-ranking, including inter-session and intra-session re-  
847 ranking. This re-ranking process improved the system precision from  
848 0.8 to 0.89. The importance of negative feedback in this process is  
849 highlighted in (Muller et al., 2000).

850 In most cases, re-ranking methods are only required to consider the top  
851 ranked initial retrieval results, e.g., most truly relevant images are included  
852 in the top- $K$  results, and  $K$  is much smaller than the number of images in the  
853 whole database. Therefore, re-ranking can be very efficient as it only needs  
854 to process a few images. More importantly, by considering and comparing  
855 the similarity using multiple information sources, the retrieval precision can  
856 be improved for further exploration and analysis.

#### 857 4.3.3. High-performance Computing

858 In addition to the above large-scale methods which belong to the fields of  
859 image processing, computer vision and machine learning, High-performance  
860 Computing (HPC) also plays an important role in medical image analytics.  
861 HPC is the use of parallel processing techniques to execute programs effi-  
862 ciently, reliably and quickly. The HPC techniques include parallel comput-  
863 ing, distributed computing, cloud computing, etc. that are useful for tackling

864 large databases. Particularly in the medical field, some large databases are  
865 usually stored in different locations and they are essential to be processed  
866 based on parallel systems.

867 Recently, HPC techniques have been widely employed for the large-scale  
868 medical retrieval. Foran et al. (Foran et al., 2011) proposed a software sys-  
869 tem based on parallel and distributed computing, namely ImageMiner, to  
870 efficiently retrieve and analyze the expression patterns of tissue microarrays  
871 (TMAs). The ImageMiner system embedded a data analysis component for  
872 efficient retrieval, i.e., DataCutter (Kumar et al., 2006), which the data pro-  
873 cessing pipeline can be composed as a network of interacting components.  
874 Images received by ImageMiner were distributed and processed by the com-  
875 putation cluster using a master-slave parallelization scheme. Subsequently,  
876 Qi et al. (Qi et al., 2014) investigated large-scale histopathological image re-  
877 trieval using the CometCloud (Kim et al., 2011), an automatic cloud frame-  
878 work that allows dynamic, on-demand federation of distributed infrastruc-  
879 tures. They first formulated the histopathological image retrieval problem as  
880 a set of heterogeneous and independent tasks. Then these tasks can be par-  
881 allelized and solved using the aggregated computational power of distributed  
882 resources. More recently, Markonis et al. (Markonis et al., 2015b) proposed  
883 solutions for the large-scale medical image analysis based on parallel com-  
884 puting and algorithm optimization. Specifically, a MapReduce framework is  
885 employed to speed up the medical image analysis in three tasks, i.e., lung  
886 texture segmentation using support vector machines, content-based medical  
887 image indexing and 3D directional wavelet analysis for solid texture classifi-  
888 cation.

889 High-performance computing can well be used to handle large-scale re-  
890 trieval tasks, especially for clinical systems, where the parallelized processing  
891 can achieve similarity retrieval in real-time. More importantly, as presented  
892 in Fig. 1, high-performance computing can be adopted in both the feature ex-  
893 traction/indexing and retrieval, which can dramatically improve the retrieval  
894 efficiency in these time-consuming steps.

895

## 896 5. Evaluation

897 After receiving similar samples from medical image retrieval systems,  
898 evaluating the retrieval performance and the whole retrieval system are also  
899 critical tasks. Especially for large-scale medical image sets, simply using class

900 labels is usually not adequate to evaluate the retrieval performance in fine-  
 901 grained levels. In the past decades, challenges and tasks such as ImageCLEF,  
 902 VISCERAL, etc. have made great efforts for the evaluation of medical im-  
 903 age retrieval (Kalpathy-Cramer et al., 2015; Langs et al., 2012). This section  
 904 reviews related work of evaluation protocols which are relevant to medical  
 905 image retrieval, including evaluation measures, criteria, and public medical  
 906 image data sets.

### 907 5.1. Evaluation Measures

908 We first introduce the evaluation measures for medical image retrieval  
 909 that can provide a quantitative analysis, comparison, and validation of dif-  
 910 ferent retrieval methods. In general, the evaluation measures in large-scale  
 911 medical image retrieval are similar with the measures in generic information  
 912 retrieval, i.e., evaluating the precision, recall, efficiency and several other  
 913 measures.

**Precision:** retrieval precision is the main indicator for performance eval-  
 uation, which can be denoted as the fraction of the images retrieved that are  
 relevant to the query image:

$$precision = \frac{|\{relevant\ images\} \cap \{retrieved\ images\}|}{|\{retrieved\ images\}|} \quad (3)$$

914 In information retrieval, precision can evaluate the capability of a method  
 915 for searching similar or relevant samples. It has also been widely used for the  
 916 evaluation of medical image retrieval methods, especially for some medical  
 917 analytical tasks where the image used as query can be better interpreted  
 918 with similar/relevant images (Li et al., 2017b; Zhang et al., 2015c,d). This  
 919 is similar to asking a colleague for help or searching similar images/patterns  
 920 in books.

Besides precision, mean average precision (MAP) is most commonly used  
 for the evaluation of retrieval methods and for the comparison of search in  
 large-scale medical image sets. MAP is relatively stable and include aspects  
 of precision and recall, as it averages over positions of all relevant items. It  
 is defined as the mean of the average precision scores of all relevant items of  
 a query averaged over all queries. The MAP can be formulated as:

$$MAP = \frac{1}{|M|} \sum_{m=1}^M \frac{1}{|K|} \sum_{k=1}^K precision(Q_{m,k}) \quad (4)$$

921 where  $M$  is the number of query images (i.e., testing data),  $K$  indicates  
 922 the top- $K$  ranked relevant images for each query image, and  $Q_{m,k}$  denotes  
 923 the top- $k$  retrieval precision of the  $m$ th query image. For large-scale retrieval  
 924 methods, the MAP can evaluate their performance with massive testing data  
 925 (e.g., hundreds to thousands of query images), and thus alleviate the bias  
 926 during precision evaluation.

**Recall:** in image retrieval, recall is the fraction of relevant retrieved images with all relevant images in databases, i.e.:

$$recall = \frac{|\{relevant\ images\} \cap \{retrieved\ images\}|}{|\{all\ relevant\ images\}|} \quad (5)$$

927 Recall reflects the sensitivity of a retrieval system, i.e., whether it can com-  
 928 pletely find all relevant samples in top- $K$  ranked results, keeping  $K$  as small  
 929 as possible. Thus, for medical retrieval tasks that need to find all relevant  
 930 samples for analysis (such as a systematic review), recall is a critical evalu-  
 931 ation criterion. Normally, recall is associated with precision, i.e., precision-  
 932 recall curve, for the evaluation and comparison of different retrieval methods  
 933 with a global view on the performance (Davis and Goadrich, 2006; Müller  
 934 et al., 2001).

**Efficiency:** as directly indexing massive images with high dimensional features are usually very time-consuming, one important evaluation indicator for large-scale retrieval is efficiency. Currently, in most large-scale retrieval cases, efficiency is denoted as the time for the feature indexing phase, i.e., given a query image (or its features), the time for returning a set of relevant images after searching in large-scale databases. For medical image retrieval with many testing images, their accumulated and average run time are the commonly used efficiency measures, where the average run time can be formulated as:

$$AvgTime = \frac{1}{M} \sum_{m=1}^M t_{m,K} \quad (6)$$

935  $t_{m,K}$  indicates the time cost of retrieving  $K$  relevant images for the  $m$ th  
 936 query image. The average/accumulated run time has been widely adopted  
 937 for the evaluation, comparison and validation of large-scale medical image  
 938 retrieval (Jiang et al., 2016a, 2015c; Zhang et al., 2015c,d). Still, run times  
 939 need to be put in relationship to hardware resources available and are thus  
 940 not always easy to interpret. Sometimes the run time for the offline parts

941 (data indexation) and the online parts (interactive search) are separately  
942 compared.

943 Additionally, there are several other commonly employed measures for  
944 medical image retrieval evaluation. For example, the precision after the first  
945  $N_R$  images are retrieved (i.e.,  $P(N_R)$ ), recall at 0.5 precision, rank first rele-  
946 vant, etc.). These measures were discussed in previous articles (Müller et al.,  
947 2001; Muller et al., 2004).

## 948 5.2. Evaluation Criteria

949 In addition to evaluation measures, the criteria of deciding similarity/relevance  
950 are also important and challenging tasks in large-scale medical image re-  
951 trieval. Here, we introduce two kinds of evaluation criteria: annotation-based  
952 and user-based, which are the commonly employed criteria in medical image  
953 retrieval.

954 **Annotation-based Criteria:** when class labels of medical images are  
955 available, their annotations are a commonly used evaluation criterion. As the  
956 class labels of all medical images in the database are provided, the similar or  
957 relevant images can be determined quickly by comparing their class labels.  
958 Thus, given testing images, the retrieval precision and recall can be mea-  
959 sured by sequentially comparing the labels between each test image and the  
960 retrieved images. Currently, several large-scale medical image retrieval cases  
961 adopted annotation-based criteria for performance evaluation. For example,  
962 Zhang et al. (Zhang et al., 2015d) evaluated the large-scale histopatholog-  
963 ical image retrieval through the class label of two type lung cancers (i.e.,  
964 adenocarcinoma and squamous carcinoma) for each image. The annotation-  
965 based evaluation criteria are only suitable for the cases that image classes are  
966 identified and the similarity of images are simply determined by class labels.

967

968 **User-based Criteria:** despite the annotation-based criteria being a sim-  
969 ple way for retrieval evaluation, it may not suitable in many practical cases of  
970 large-scale medical image retrieval. One reason is that the annotation of med-  
971 ical images is usually hard to obtain. Some medical images are still classified  
972 and do not have unified classification rules. Moreover, annotating every med-  
973 ical image in large databases is extremely labor expensive,time-consuming,  
974 and sometimes impossible. Another reason is the similarity/relevance mea-  
975 sure. In large-scale medical image retrieval, one query image may have thou-  
976 sands of images with the same label. For some analytical tasks, simply using  
977 class labels is not adequate to identify relevant images.

978 Compared with annotation-based criteria, users or domain experts can  
979 provide more fine-grained retrieval evaluations in the form of relevance judge-  
980 ments for specific tasks. Many medical image retrieval systems have em-  
981 ployed users for the performance evaluation. In general, users can observe  
982 the retrieved images and assign them with different relevance levels during  
983 evaluation. For example, the medical ImageCLEF challenges used three lev-  
984 els of relevance, i.e., relevant, partly-relevant, and non-relevant (Kalpathy-  
985 Cramer et al., 2011; Müller et al., 2012, 2009). These relevance judgments  
986 were employed for the retrieval performance evaluation of the database with  
987 300,000 medical images. Besides ImageCLEF challenges, considering neu-  
988 rons is usually hard to classify and identify, Wan et al. (Wan et al., 2015)  
989 asked two users for the visual comparison of morphological neuron retrieval  
990 results. In medical image retrieval, user-based criteria rely on user’s domain  
991 knowledge and may be partly subjective based on the user’s background.  
992 Thus, the retrieval results are usually judged by two or more users for more  
993 reliable evaluation.

994 The evaluation of system design also plays an important role in medi-  
995 cal image retrieval, especially for the retrieval systems where users are in-  
996 teractively involved. Markonis et al. (Markonis et al., 2015a) reported the  
997 user-oriented evaluation of a text- and content-based medical image retrieval  
998 system. In total, 16 radiologists participated in the user tests with a work-  
999 ing image retrieval system in an iterative manner. Such analyses in clinical  
1000 practice are really needed to advance the practical use of image retrieval in  
1001 hospitals

### 1002 5.3. Public Datasets

1003 With the increasing availability of digital imaging techniques, a large  
1004 number of medical images are generated and well organized in many repos-  
1005 itories. Some of the repositories are publicly available for users and re-  
1006 searchers. The medical image repositories usually include thousands to mil-  
1007 lions of images. Images are collected for different purposes, such as cancer  
1008 grading/staging and treatment planning. We briefly introduce some of the  
1009 public data sets that are widely used for medical image retrieval:

- 1010 • ImageCLEF (ImageCLEF): ImageCLEF provides an evaluation forum  
1011 for the cross-language annotation and retrieval of images. ImageCLEF  
1012 has held 14 years of medical image retrieval challenges, with the number



1013 of images in the dataset having increased from 6,000 to 300,000 ([Kalpathy-](#)  
1014 [Cramer et al., 2015](#)). The datasets in ImageCLEF include multiple  
1015 modalities of medical images, e.g., radiology, microscopy and also gen-  
1016 eral photography.

1017 • [DDSM \(of South Florida\)](#): The digital database for screening mammog-  
1018 raphy (DDSM) is a public mammogram database. It includes 2,604  
1019 breast cases and every case consists of four views, with two cranio-  
1020 caudal views and two mediolateral oblique views. The mammographic  
1021 masses have different shapes, sizes, margins and breast densities as  
1022 well as the patient race and age, which provide rich information for  
1023 diagnosis.

1024 • [MedPix \(of Medicine\)](#): MedPix is a fully web-enabled cross-platform  
1025 database, integrating images and text information. This medical image  
1026 database includes over 53,000 indexed and curated images, from more  
1027 than 13,000 patients. The merit of this database is that it records  
1028 detailed descriptions of patients and their corresponding diagnosis.

1029 • [TCGA \(Institute, a\)](#): The Cancer Genome Atlas (TCGA) collects a  
1030 huge amount of cancer images (currently around 10,000,000 images  
1031 and increasing quickly) from multiple projects funded by National Can-  
1032 cer Institute. It records many types of cancer images, including but not  
1033 limited to, brain, esophageal, lung, thyroid and rectum. All TCGA  
1034 data reside in the Genomic Data Commons ([Institute, b](#)).

1035 • [TCIA \(TCIA\)](#): The Cancer Imaging Archive (TCIA) is organized into  
1036 collections with a variety of cancer types and/or anatomical areas. Sim-  
1037 ilar to TCGA, it collects cancer images from many projects and insti-  
1038 tutes. The cancer types include breast, prostate, liver, lung, brain, etc.  
1039 and the image modalities include CT, MR, PET and others.

1040 • [VISCERAL \(VISCERAL\)](#): VISCERAL is the abbreviation for Visual  
1041 Concept Extraction Challenge in Radiology, which provides a bench-  
1042 mark for the retrieval in the medical domain. This dataset consists  
1043 2,311 medical 3D volumes originating from various modalities (CT,  
1044 MRT1, MRT2 with and without contrast agent) and each volume con-  
1045 sists 200 – 2000 images (slices). The VISCERAL project has organized

Public data sets	Number of images or or size	Image category
ImageCLEF ( <a href="#">ImageCLEF</a> )	300,000	Multi-modalities
DDSM ( <a href="#">of South Florida</a> )	10,480, 231GB	Mammogram
MedPix ( <a href="#">of Medicine</a> )	53,000	Multi-modalities
TCGA ( <a href="#">Institute, a</a> )	470TB	Cancer Images, Multi-modalities
TCIA ( <a href="#">TCIA</a> )	10,000,000, 3TB	Cancer Images, Multi-modalities
Retinopathy ( <a href="#">EyePACS</a> )	35,000, 82GB	Retinal Photographs
DREAM ( <a href="#">Bionetworks</a> )	640,000	Screening Mammograms
VISCERAL ( <a href="#">VISCERAL</a> )	2,300	3D CT, MRI volume
LIDC-IDRI ( <a href="#">Armato III et al., 2011</a> )	240,000, 124GB	Lung CT, DX, and CR
ADNI ( <a href="#">of Southern California</a> )	Unknown	Alzheimer’s MR, PET, etc
NBIA ( <a href="#">NBIA</a> )	76,000	Cancer Images, Multi-modalities
CAMELYON 17 ( <a href="#">, DIAG</a> )	1,000, 2TB	Whole-slide Histopathological Images
PubMed Center ( <a href="#">NCBI</a> )	4,000,000	Multi-modalities
NLST ( <a href="#">Institute, c</a> )	76,000	Lung CT, Pathology Images

**Table 3:** Current publicly available medical image data sets.

1046 several challenges, workshops and provided multiple benchmarks re-  
1047 lated to large-scale data in medical image analysis and retrieval ([Langs](#)  
1048 [et al., 2012](#); [Müller et al., 2014](#); [Zhang et al., 2015a](#)).

1049 In addition to the above data sets, [Table 3](#) presents a summary of publicly  
1050 available data sets with many medical images, including number of images,  
1051 size and categories if available. Due to the fast growth of medical images, we  
1052 only provide a small subset of commonly used data sets in [Table 3](#).

## 1053 6. Applications

1054 After reviewing the above large-scale techniques, we introduce their ap-  
1055 plications for medical image analytics in this section. Large-scale retrieval  
1056 methods have demonstrated impressive improvement on many medical image  
1057 types, including CT, MRI, X-ray, microscopy and others. In the following, we  
1058 illustrate their applications in clinical diagnosis, cancer grading, and neuron  
1059 exploration.

### 1060 6.1. Mammographic Retrieval and Segmentation

1061 Breast cancer remains the second leading cause of cancer-related death  
1062 among women ([Society, 2013](#)). Early diagnosis based on mammography is a  
1063 widely adopted approach to improving the chances of recovery, which is recog-  
1064 nized as a gold standard for breast cancer detection by the American Cancer  
1065 Society ([Society, 2013](#)). However, the detection of masses in a mammogram  
1066 is a challenging task, as masses have a large variation in shape, margin, and

1067 size. They are often indistinguishable from surrounding tissue (Cheng et al.,  
1068 2006; Oliver et al., 2010). For an undetected mammogram, computer-aided  
1069 diagnosis (CAD) with content-based image retrieval (CBIR) is an effective  
1070 solution by returning a limited number of the most similar mammograms in  
1071 the pre-built image database, where the retrieved mammograms were already  
1072 annotated with the class labels of mass and normal. Nevertheless, with the  
1073 ever increasing number of mammograms generated and added to the pre-  
1074 built database, scalable CBIR techniques have become one of the important  
1075 problems for mammogram based breast cancer diagnosis (Langs et al., 2012).

1076 Jiang et al. (Jiang et al., 2015c) successfully solved the scalable mammo-  
1077 gram retrieval problem based on a vocabulary tree with adaptive weighting.  
1078 For a query with a mammographic region of interest (ROI), it can achieve  
1079 efficient retrieval in a dataset with 11,553 ROIs. Specifically, in the experi-  
1080 ment, this method reported an 88.4% retrieval precision with 500 mass ROIs  
1081 and 500 normal ROIs as queries. This demonstrates good accuracy com-  
1082 pared with other methods including NMI (Tourassi et al., 2007), BoW (André  
1083 et al., 2012), and VocTree (Nister and Stewenius, 2006). The method also  
1084 achieved highest classification accuracy (90.8%) for whether the query ROIs  
1085 are masses or normal. Additionally, this method is 3 to 10 times faster than  
1086 other methods and the advantage is larger when the size of image database  
1087 increases.

1088 (Jiang et al., 2016b) propose to learn online shape and appearance priors  
1089 via image retrieval, i.e., setting an input mass as the query, its visually  
1090 similar training masses can be obtained by image retrieval. Then, the query  
1091 mass can be segmented using the retrieval priors and graph cuts. Extensive  
1092 experiments on a mammography database demonstrate that the method can  
1093 improve the segmentation accuracy and outperform several widely used mass  
1094 segmentation methods.

## 1095 6.2. Cell-Level Histopathological Image Analysis

1096 Histopathological image analysis is widely used for cancer grading. Com-  
1097 pared to mammography, CT and others, histopathology slides provide more  
1098 comprehensive information for diagnosis and the diseases are analyzed by  
1099 detecting tissue and cells in lesions (Gurcan et al., 2009). On the other hand  
1100 an invasive biopsy is necessary, which is often tried to be avoided. CBIR sys-  
1101 tems are commonly employed to analyze histopathological images (Caicedo  
1102 et al., 2009, 2011; Doyle et al., 2007). In CBIR systems, the returned visually  
1103 similar images can be used to identify and classify the query images (e.g.,

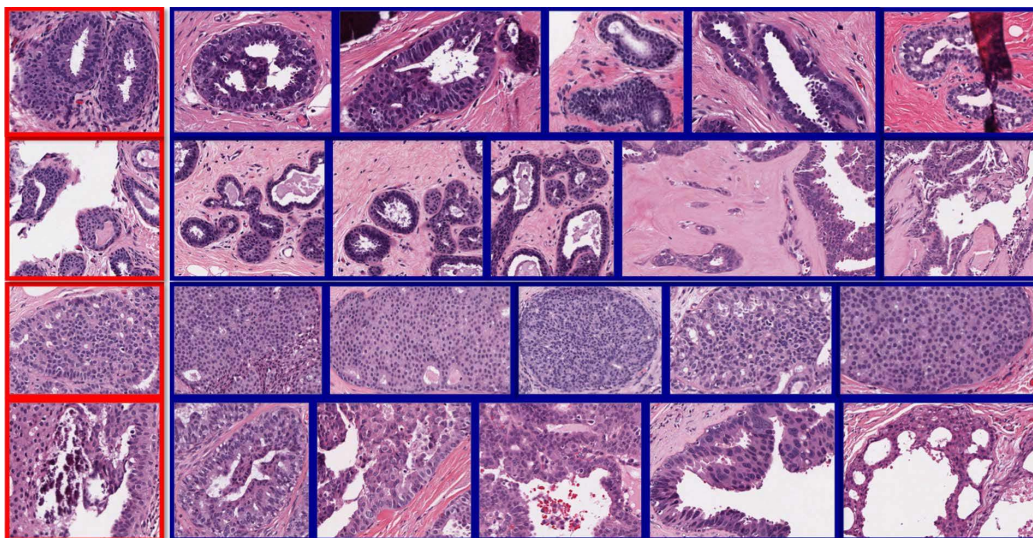


**Figure 8:** Examples of hashing-based histopathological image retrieval illustrated in (Zhang et al., 2015c) (query marked in red and retrieved images marked in blue). The first two rows are benign tissue; the last two rows are malignant tissue.

1104 classifying them as benign or malignant), and further assist pathologists to  
 1105 describe the tissue samples.

1106 Hashing methods were first employed by Zhang et al. (Zhang et al., 2015c,  
 1107 2014) to tackle large histopathological image databases for CBIR. They de-  
 1108 signed a comprehensive CBIR framework to analyze histopathological images  
 1109 by leveraging high-dimensional texture features and kernelized hashing with  
 1110 supervised information. In the experiment, this hashing method demon-  
 1111 strated significant improvement in histopathological image classification and  
 1112 retrieval tasks. Compared to methods such as SVM (Caicedo et al., 2009),  
 1113 Adaboost (Doyle et al., 2012), KNN (Tabesh et al., 2007), and Graph Em-  
 1114 bedding (Basavanhally et al., 2010), its accuracy was 5 to 10 percent higher.  
 1115 The method achieved histopathological retrieval for 700-900 images within  
 1116 0.01 seconds (3121 images in the database), which is 1000 times faster than  
 1117 the given baseline. Fig. 8 illustrates four queries (two benign images, two  
 1118 malignant images) and their corresponding top five retrieval results based  
 1119 on this hashing-based CBIR framework. Despite the difference between be-  
 1120 nign and malignant images being subtle, the proposed method is effective  
 1121 to retrieve images in the same category. The authors extended the CBIR

1122 system for more accurate diagnosis by examining the cells in histopathology  
1123 images (Zhang et al., 2015d). As each histopathology image usually includes  
1124 thousands of cells, examining every cell by traditional retrieval methods is al-  
1125 most impossible when the image databases are large. Thus, a hashing-based  
1126 framework is proposed that enables cell-level analysis in real-time with high  
1127 accuracy, i.e., indexing 96,000 cells within 1.68 seconds (the whole database  
1128 includes 484,136 cells), and achieving 87.3% accuracy for the classification of  
1129 histopathology lung images (i.e., two types of lung cancers, adenocarcinoma  
1130 or squamous carcinoma).

1131 In histopathological image analysis, it is a common practice to employ  
1132 multiple features to improve performance. To embed multiple features in  
1133 a hashing framework, Jiang et al. (Jiang et al., 2015b, 2016a) employed  
1134 joint kernel-based supervised hashing (JKSH) for scalable histopathological  
1135 image analysis, where multiple features are linearly combined by individual  
1136 kernels (Liu et al., 2014c). Experiments on breast cancer histopathology  
1137 images demonstrate the effectiveness in both retrieval and classification.

### 1138 *6.3. Exploration of a Neuron Databases*

1139 Analyzing single neuron properties, such as cell types, brain regions, func-  
1140 tions and development stages is usually a fundamental task to understand  
1141 the nervous system and brain mechanisms. In general, neuron morphology  
1142 plays a major role in determining the neuron’s functional and physiologi-  
1143 cal properties. Recent approaches in neuroscience (e.g., BigNeuron (big, a))  
1144 have facilitated the research in neuron morphology. An increasing number of  
1145 neurons are reconstructed and added to the public repositories (big, b; Neu-  
1146 roMorpho). Therefore, given an unknown neuron, it is reasonable to explore  
1147 its properties through the morphological retrieval in neuron databases.

1148 Conjeti et al. (Conjeti et al., 2016b; Mesbah et al., 2015) developed an  
1149 advanced tool for morphological search and retrieval in large-scale neurosci-  
1150 entific image databases, namely Neuron-Miner. Neuron-Miner first employs  
1151 quantitative measurements as neuron features, such as soma surface, the  
1152 number of branches and the neuron’s total length. Then, it adopts a novel  
1153 hashing method, i.e., hashing forests, to compact the features into binary  
1154 codes. In the experiment, Neuron-Miner demonstrates the effectiveness in  
1155 morphological retrieval with a database including 31,266 neurons. **Given a  
1156 query, this tool is able to return several visually similar neurons from the  
1157 database. The ground truth (using normalized Euclidean distance) shows  
1158 that returned neurons are relevant to the query.**

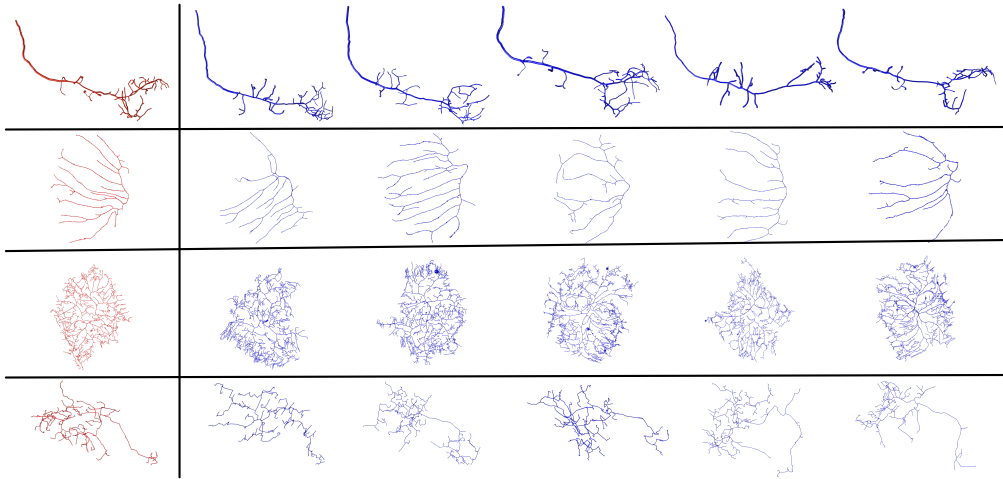


**Figure 9:** Results of morphological neuron retrieval shown in (Li et al., 2017a). For each neuron on the left (red), the top-5 retrieved neurons on the right (blue) are shown. This illustrates the morphological similarity between query neurons and retrieved neurons.

1159 More recently, Li et al. (Li et al., 2017a, 2016) explored large-scale mor-  
 1160 phological neuron databases based on a novel search strategy, the maxi-  
 1161 mum inner product search (MIPS). Based on MIPS, nonlinear hashing func-  
 1162 tions are learned by embedding the inner code product rather than the con-  
 1163 ventional Hamming distance. The nonlinear hashing functions are partic-  
 1164 ularly suitable for the morphological neuron retrieval problem, since the  
 1165 neurons’ tree-topological structure makes them hard to be discriminative  
 1166 in low-dimensional linear space. Fig. 9 demonstrates that the MIPS-based  
 1167 method is able to retrieve morphologically similar neurons in the large-scale  
 1168 database. To evaluate the retrieval precision, it employed projection neurons  
 1169 in the olfactory bulb as queries. The retrieval results validated that most  
 1170 returned neurons have the same properties as the queries (with a reported  
 1171 90.48% average precision in the top-5 relevant neurons). Additionally, the  
 1172 authors demonstrated the application of morphological retrieval in neuron  
 1173 exploration. By collecting properties of the top- $K$  relevant neurons (e.g.,  
 1174 a neurons’ brain regions, cell types, transmitters). Properties of the query  
 1175 neuron can be inferred in real-time based on this MIPS hashing framework.

## 1176 7. Future Directions

1177 After reviewing the above methods and applications of large-scale med-  
1178 ical image analytics, we discuss possible future directions in this section.  
1179 Despite varieties of advanced large-scale techniques being employed for re-  
1180 trieval, there are still many directions to explore and improve the retrieval  
1181 performance.

1182 **Multi-features:** in general, only employing a single kind of feature is  
1183 not enough to represent and discriminate medical images. Especially when  
1184 a database is large, the difference with some irrelevant images can be sub-  
1185 tle. One intuitive solution is using multiple features to represent each image,  
1186 e.g., local, holistic, and texture features. These features can be fused and  
1187 embedded in a large-scale retrieval framework. According to existing work,  
1188 multi-feature fusion can be conducted on three levels during retrieval, i.e.,  
1189 feature level (Atrey et al., 2010), training level (Liu et al., 2014c), and deci-  
1190 sion level (Zhang et al., 2012). Jiang et al. (Jiang et al., 2016a) fuse three  
1191 types of features (SIFT (Lowe, 2004), HOG (Dalal and Triggs, 2005), and  
1192 GIST (Oliva and Torralba, 2001)) in the training level when learning hashing  
1193 functions; Zhang et al. (Zhang et al., 2016a) employ a graph-based query-  
1194 specific fusion approach to integrating local and holistic features at the deci-  
1195 sion level. Despite the two methods having achieved good performance, these  
1196 are far from enough for large-scale medical image retrieval. With the ever-  
1197 increasing techniques in feature representation, employing more features to  
1198 retrieve complex medical images is a clear trend (e.g. the ImageCLEF med-  
1199 ical image retrieval tasks in recent years). However, as diverse features have  
1200 different meanings and representations, deciding on the importance of each  
1201 feature is a challenging task. User specified feature importance is usually  
1202 not reliable, and automatically computing each feature’s importance is time-  
1203 consuming, especially when dealing with many features in a large database.  
1204 Thus, successfully handling multi-feature fusion in a large-scale database fur-  
1205 ther improves the accuracy and efficiency of medical image retrieval.

1206 **Online updating:** as more medical images are being generated, the size  
1207 of the corresponding databases are continuously increasing. For example, the  
1208 aforementioned ImageCLEF database increased the number of images from  
1209 600 to 300,000, and the NeuroMorpho database usually releases 1,000 to  
1210 2,000 reconstructed neuron cells in each update. The newly added images  
1211 should be considered to train new models for retrieval, since employing more  
1212 training data can accordingly improve the retrieval accuracy. However, if we

1213 re-train a large-scale model every time from scratch, using both the original  
1214 and the newly added images, it is time-consuming and adversely affects the  
1215 efficiency of medical retrieval. On the other side, when the medical image  
1216 databases are extremely large (e.g., including millions of images), current  
1217 storage techniques are not able to arrange and process all the images within  
1218 one batch. More importantly, both the vocabulary tree and hashing based  
1219 methods cannot efficiently train models for the huge amount of images at a  
1220 given time, e.g., building a hierarchical tree or learning hashing functions with  
1221 millions of feature vectors. To tackle these problems, one possible solution  
1222 is to divide huge databases into several batches, and then develop an online  
1223 updating strategy to train the retrieval model with one-by-one image batches  
1224 in a streaming manner. The newly added images can also be treated as  
1225 a batch to update the retrieval model. Currently, several online hashing  
1226 methods have been developed for computer vision tasks (Cakir and Sclaroff,  
1227 2015; Huang et al., 2013; Leng et al., 2015). In medical image analytics,  
1228 the merit of the online updating strategy is beneficial in the future with a  
1229 continuously increasing number of images and extremely large databases.

1230 **Bringing humans in the loop:** for the retrieval of large-scale medical  
1231 image databases, lacking label information is the main limitation to achieve  
1232 good retrieval results. As medical images usually have different modalities  
1233 and appearances, their intra-class variations can be large, and their inter-  
1234 class variations can be small. The image labels are useful to handle this  
1235 problem, since it can embed supervised information in retrieval models and  
1236 bridge the low-level features with high-level image semantics. However, label-  
1237 ing images is not an easy task. Especially for some medical images, assigning  
1238 their labels requires domain experts with proper training. Crowdsourcing can  
1239 be used when very precisely defined tasks allow for quick training times (Fon-  
1240 cubierta Rodríguez and Müller, 2012). Deciding whether a histopathology  
1241 image contains benign or malignant lesions is complex and time-consuming,  
1242 for example. Moreover, large-scale databases make this task even harder.  
1243 To tackle these problems, one feasible solution is to bring humans in the  
1244 retrieval loop. They can interactively give feedback to improve the retrieval  
1245 performance (Feng et al., 2013; Rui et al., 1998). After acquiring a set of  
1246 similar images from unsupervised retrieval, users/domain experts can specify  
1247 images relevant to the query and those that are not. Such feedback can be  
1248 returned to the retrieval system to improve the final results (Bulo et al., 2011;  
1249 Sahbi et al., 2007). The feedback can be treated as supervised information  
1250 but it is more efficient than labeling all medical images. Theoretically, such



1251 an interactive strategy can achieve two goals: 1) it presents retrieval results  
1252 to users/domain experts to help them analyze medical images; 2) it receives  
1253 and uses the interactive feedback to improve the retrieval system.

## 1254 **8. Conclusions**

1255 In this review, we summarize recent advances of large-scale retrieval for  
1256 medical image analytics. By introducing the pipeline of large-scale retrieval,  
1257 we presented a comprehensive review of relevant techniques that can improve  
1258 the efficiency and accuracy of medical image analysis, including feature rep-  
1259 resentation, feature indexing and searching. We also reviewed clinical appli-  
1260 cations and discussed the future directions of large-scale medical analytics.  
1261 With the ever-increasing amount of newly generated medical images, we be-  
1262 lieve that the algorithms and methods of large-scale medical image analytics  
1263 will lead to new ideas for knowledge discovery and decision support.

1264 Currently, only few systems have been exposed to detailed user test-  
1265 ing (Markonis et al., 2015a) and such user tests are clearly needed for very  
1266 large scale systems. Many currently CBIR systems only use small databases  
1267 and not update mechanisms and this is required for real application including  
1268 an integration of the systems into the standard clinical workflow, which is  
1269 often neglected. Many technical approaches are now available for large-scale  
1270 applications but more work is needed to actually integrate the tools for clin-  
1271 ical impact, an this includes the use of deep learning and explaining these  
1272 results to physicians.

## 1273 **Acknowledgement**

1274 This work is partially supported by the National Science Foundation un-  
1275 der grant ABI-1661280, CNS-1629913 and IIP-1439695.

## 1276 **References**

1277 , a. Bigneuron project. <http://www.alleninstitute.org/bigneuron/>. Accessed June  
1278 28, 2016.

1279 , b. Bigneuron released data. <https://github.com/BigNeuron/Data/releases>. Accessed  
1280 June 28, 2016.

- 1281 , 2010. Riding the wave: How europe can gain from the rising tide of scientific data.  
1282 Submission to the European Commission, available online at [http://cordis.europa.](http://cordis.europa.eu/fp7/ict/e-infrastructure/docs/hlg-sdi-report.pdf)  
1283 [eu/fp7/ict/e-infrastructure/docs/hlg-sdi-report.pdf](http://cordis.europa.eu/fp7/ict/e-infrastructure/docs/hlg-sdi-report.pdf). URL: [http://cordis.](http://cordis.europa.eu/fp7/ict/e-infrastructure/docs/hlg-sdi-report.pdf)  
1284 [europa.eu/fp7/ict/e-infrastructure/docs/hlg-sdi-report.pdf](http://cordis.europa.eu/fp7/ict/e-infrastructure/docs/hlg-sdi-report.pdf).
- 1285 Agarwal, M., Mostafa, J., 2011. Content-based image retrieval for alzheimer’s disease  
1286 detection, in: Content-Based Multimedia Indexing (CBMI), 2011 9th International  
1287 Workshop on, IEEE. pp. 13–18.
- 1288 Akgül, C.B., Rubin, D.L., Napel, S., Beaulieu, C.F., Greenspan, H., Acar, B., 2011.  
1289 Content-based image retrieval in radiology: current status and future directions. *Journal*  
1290 *of Digital Imaging* 24, 208–222.
- 1291 André, B., Vercauteren, T., Buchner, A.M., Wallace, M.B., Ayache, N., 2012. Learning  
1292 semantic and visual similarity for endomicroscopy video retrieval. *IEEE Transactions*  
1293 *on Medical Imaging* 31, 1276–1288.
- 1294 Antani, S.K., Deserno, T.M., Long, L.R., Güld, M.O., Neve, L., Thoma, G.R., 2007. In-  
1295 terfacing global and local cbir systems for medical image retrieval, in: *Bildverarbeitung*  
1296 *für die Medizin 2007*. Springer, pp. 166–171.
- 1297 Antipov, G., Berrani, S.A., Ruchaud, N., Dugelay, J.L., 2015. Learned vs. hand-crafted  
1298 features for pedestrian gender recognition, in: *Proceedings of the 23rd ACM Interna-*  
1299 *tional Conference on Multimedia*, ACM. pp. 1263–1266.
- 1300 Armato III, S.G., McLennan, G., Bidaut, L., McNitt-Gray, M.F., Meyer, C.R., Reeves,  
1301 A.P., Zhao, B., Aberle, D.R., Henschke, C.I., Hoffman, E.A., et al., 2011. The lung  
1302 image database consortium (lidc) and image database resource initiative (idri): a com-  
1303 pleted reference database of lung nodules on ct scans. *Medical Physics* 38, 915–931.
- 1304 Atrey, P.K., Hossain, M.A., El Saddik, A., Kankanhalli, M.S., 2010. Multimodal fusion  
1305 for multimedia analysis: a survey. *Multimedia Systems* 16, 345–379.
- 1306 Babenko, A., Lempitsky, V., 2015. Aggregating local deep features for image retrieval, in:  
1307 *Proceedings of the IEEE international conference on computer vision*, pp. 1269–1277.
- 1308 Bailey, D.L., Townsend, D.W., Valk, P.E., Maisey, M.N., 2005. *Positron emission tomog-*  
1309 *raphy*. Springer.
- 1310 Bar, Y., Diamant, I., Wolf, L., Lieberman, S., Konen, E., Greenspan, H., 2015. Chest  
1311 pathology detection using deep learning with non-medical training, in: *2015 IEEE 12th*  
1312 *International Symposium on Biomedical Imaging (ISBI)*, IEEE. pp. 294–297.
- 1313 Basavanthally, A.N., Ganesan, S., Agner, S., Monaco, J.P., Feldman, M.D., Tomaszewski,  
1314 J.E., Bhanot, G., Madabhushi, A., 2010. Computerized image-based detection and  
1315 grading of lymphocytic infiltration in her2+ breast cancer histopathology. *IEEE Trans-*  
1316 *actions on Biomedical Engineering* 57, 642–653.

- 1317 Bay, H., Ess, A., Tuytelaars, T., Van Gool, L., 2008. Speeded-up robust features (surf).  
1318 Computer Vision and Image Understanding 110, 346–359.
- 1319 Bengio, Y., 2009. Learning deep architectures for ai. Foundations and trends® in Machine  
1320 Learning 2, 1–127.
- 1321 Bengio, Y., Courville, A.C., Vincent, P., 2012. Unsupervised feature learning and deep  
1322 learning: A review and new perspectives. CoRR, abs/1206.5538 1.
- 1323 Bionetworks, S., . The digital mammography dream challenge. [https://www.synapse.  
1324 org/Synapse:syn4224222/wiki/](https://www.synapse.org/Synapse:syn4224222/wiki/). Accessed October 23, 2016.
- 1325 Bourlard, H., Kamp, Y., 1988. Auto-association by multilayer perceptrons and singular  
1326 value decomposition. Biological Cybernetics 59, 291–294.
- 1327 Brosch, T., Tam, R., Initiative, A.D.N., et al., 2013. Manifold learning of brain mris  
1328 by deep learning, in: International Conference on Medical Image Computing and  
1329 Computer-Assisted Intervention, Springer. pp. 633–640.
- 1330 Bulo, S.R., Rabbi, M., Pelillo, M., 2011. Content-based image retrieval with relevance  
1331 feedback using random walks. Pattern Recognition 44, 2109–2122.
- 1332 Bunte, K., Biehl, M., Jonkman, M.F., Petkov, N., 2011. Learning effective color features  
1333 for content based image retrieval in dermatology. Pattern Recognition 44, 1892–1902.
- 1334 Cai, W., Liu, S., Wen, L., Eberl, S., Fulham, M.J., Feng, D., 2010. 3d neurological image  
1335 retrieval with localized pathology-centric cmrglc patterns, in: 2010 IEEE International  
1336 Conference on Image Processing, IEEE. pp. 3201–3204.
- 1337 Caicedo, J.C., Cruz, A., Gonzalez, F.A., 2009. Histopathology image classification using  
1338 bag of features and kernel functions, in: Conference on Artificial Intelligence in Medicine  
1339 in Europe, Springer. pp. 126–135.
- 1340 Caicedo, J.C., Gonzalez, F.A., Romero, E., 2007. Content-based medical image retrieval  
1341 using low-level visual features and modality identification, in: Workshop of the Cross-  
1342 Language Evaluation Forum for European Languages, Springer. pp. 615–622.
- 1343 Caicedo, J.C., González, F.A., Romero, E., 2011. Content-based histopathology image  
1344 retrieval using a kernel-based semantic annotation framework. Journal of Biomedical  
1345 Informatics 44, 519–528.
- 1346 Cakir, F., Sclaroff, S., 2015. Adaptive hashing for fast similarity search, in: Proceedings  
1347 of the IEEE International Conference on Computer Vision, pp. 1044–1052.
- 1348 Cao, Y., Steffey, S., He, J., Xiao, D., Tao, C., Chen, P., Müller, H., 2014. Medical image  
1349 retrieval: A multimodal approach. Cancer Informatics 13, 125.

- 1350 Cheng, H., Shi, X., Min, R., Hu, L., Cai, X., Du, H., 2006. Approaches for automated  
1351 detection and classification of masses in mammograms. *Pattern Recognition* 39, 646–  
1352 668.
- 1353 Chenouard, N., Unser, M., 2011. 3d steerable wavelets and monogenic analysis for bioimag-  
1354 ing, in: 2011 IEEE International Symposium on Biomedical Imaging: From Nano to  
1355 Macro, IEEE. pp. 2132–2135.
- 1356 Ciompi, F., de Hoop, B., van Riel, S.J., Chung, K., Scholten, E.T., Oudkerk, M., de Jong,  
1357 P.A., Prokop, M., van Ginneken, B., 2015. Automatic classification of pulmonary  
1358 peri-fissural nodules in computed tomography using an ensemble of 2d views and a  
1359 convolutional neural network out-of-the-box. *Medical Image Analysis* 26, 195–202.
- 1360 Collins, D.J., Padhani, A.R., 2004. Dynamic magnetic resonance imaging of tumor perfu-  
1361 sion. *IEEE Engineering in Medicine and Biology Magazine* 23, 65–83.
- 1362 Conjeti, S., Katouzian, A., Kazi, A., Mesbah, S., Beymer, D., Syeda-Mahmood, T.F.,  
1363 Navab, N., 2016a. Metric hashing forests. *Medical Image Analysis* .
- 1364 Conjeti, S., Mesbah, S., Negahdar, M., Rautenberg, P.L., Zhang, S., Navab, N., Katouzian,  
1365 A., 2016b. Neuron-miner: An advanced tool for morphological search and retrieval in  
1366 neuroscientific image databases. *Neuroinformatics* 14, 369–385.
- 1367 Dalal, N., Triggs, B., 2005. Histograms of oriented gradients for human detection, in:  
1368 2005 IEEE Computer Society Conference on Computer Vision and Pattern Recognition  
1369 (CVPR'05), IEEE. pp. 886–893.
- 1370 Davis, J., Goadrich, M., 2006. The relationship between precision-recall and roc curves,  
1371 in: Proceedings of the 23rd international conference on Machine learning, ACM. pp.  
1372 233–240.
- 1373 Deng, J., Dong, W., Socher, R., Li, L.J., Li, K., Fei-Fei, L., 2009. Imagenet: A large-  
1374 scale hierarchical image database, in: Computer Vision and Pattern Recognition, 2009.  
1375 CVPR 2009. IEEE Conference on, IEEE. pp. 248–255.
- 1376 Depeursinge, A., Fischer, B., Müller, H., Deserno, T.M., 2011. Suppl 1: Prototypes for  
1377 content-based image retrieval in clinical practice. *The open medical informatics journal*  
1378 5, 58.
- 1379 Depeursinge, A., Müller, H., 2010. Fusion techniques for combining textual and visual  
1380 information retrieval, in: ImageCLEF. Springer, pp. 95–114.
- 1381 (DIAG), D.I.A.G., . The camelyon challenge. [https://camelyon17.grand-challenge.](https://camelyon17.grand-challenge.org/)  
1382 [org/](https://camelyon17.grand-challenge.org/). Accessed March 23, 2017.
- 1383 Doi, K., 2014. Current status and future potential of computer-aided diagnosis in medical  
1384 imaging. *The British journal of radiology* 78.

- 1385 Donahue, J., Jia, Y., Vinyals, O., Hoffman, J., Zhang, N., Tzeng, E., Darrell, T., 2014.  
1386 Decaf: A deep convolutional activation feature for generic visual recognition., in: ICML,  
1387 pp. 647–655.
- 1388 Douze, M., Jégou, H., Sandhawalia, H., Amsaleg, L., Schmid, C., 2009. Evaluation of  
1389 gist descriptors for web-scale image search, in: Proceedings of the ACM International  
1390 Conference on Image and Video Retrieval, ACM. p. 19.
- 1391 Doyle, S., Feldman, M., Tomaszewski, J., Madabhushi, A., 2012. A boosted bayesian  
1392 multiresolution classifier for prostate cancer detection from digitized needle biopsies.  
1393 IEEE Transactions on Biomedical Engineering 59, 1205–1218.
- 1394 Doyle, S., Hwang, M., Naik, S., Feldman, M., Tomaszewski, J., Madabhushi, A., 2007.  
1395 Using manifold learning for content-based image retrieval of prostate histopathology,  
1396 in: MICCAI 2007 Workshop on Content-based Image Retrieval for Biomedical Image  
1397 Archives: Achievements, Problems, and Prospects, Citeseer. pp. 53–62.
- 1398 Everingham, M., Van Gool, L., Williams, C.K., Winn, J., Zisserman, A., 2010. The  
1399 pascal visual object classes (voc) challenge. International journal of computer vision  
1400 88, 303–338.
- 1401 EyePACS, . Diabetic retinopathy detection. [https://www.kaggle.com/c/  
1402 diabetic-retinopathy-detection/](https://www.kaggle.com/c/diabetic-retinopathy-detection/). Accessed October 23, 2016.
- 1403 Fan, L., 2013. Supervised binary hash code learning with jensen shannon divergence, in:  
1404 Proceedings of the IEEE International Conference on Computer Vision, pp. 2616–2623.
- 1405 Fang, R., Pouyanfar, S., Yang, Y., Chen, S.C., Iyengar, S., 2016. Computational health  
1406 informatics in the big data age: a survey. ACM Computing Surveys (CSUR) 49, 12.
- 1407 Feng, D., Siu, W.C., Zhang, H.J., 2013. Multimedia information retrieval and man-  
1408 agement: Technological fundamentals and applications. Springer Science & Business  
1409 Media.
- 1410 Feulner, J., Zhou, S.K., Angelopoulou, E., Seifert, S., Cavallaro, A., Hornegger, J., Co-  
1411 maniciu, D., 2011. Comparing axial ct slices in quantized n-dimensional surf descriptor  
1412 space to estimate the visible body region. Computerized Medical Imaging and Graphics  
1413 35, 227–236.
- 1414 Filipczuk, P., Fevens, T., Krzyżak, A., Monczak, R., 2013. Computer-aided breast cancer  
1415 diagnosis based on the analysis of cytological images of fine needle biopsies. IEEE  
1416 Transactions on Medical Imaging 32, 2169–2178.
- 1417 Fischl, B., 2012. Freesurfer. Neuroimage 62, 774–781.
- 1418 Foncubierta-Rodríguez, A., García Seco de Herrera, A., Müller, H., 2013. Medical image  
1419 retrieval using bag of meaningful visual words: unsupervised visual vocabulary pruning  
1420 with pls, in: Proceedings of the 1st ACM International Workshop on Multimedia  
1421 Indexing and Information Retrieval for Healthcare, ACM. pp. 75–82.

- 1422 Foncubierta Rodríguez, A., Müller, H., 2012. Ground truth generation in medical imaging:  
1423 a crowdsourcing-based iterative approach, in: Proceedings of the ACM multimedia 2012  
1424 workshop on Crowdsourcing for multimedia, ACM. pp. 9–14.
- 1425 Foran, D.J., Yang, L., Chen, W., Hu, J., Goodell, L.A., Reiss, M., Wang, F., Kurc, T., Pan,  
1426 T., Sharma, A., et al., 2011. Imageminer: a software system for comparative analysis  
1427 of tissue microarrays using content-based image retrieval, high-performance computing,  
1428 and grid technology. *Journal of the American Medical Informatics Association* 18, 403–  
1429 415.
- 1430 Fukunaga, K., 2013. Introduction to statistical pattern recognition. Academic press.
- 1431 Gionis, A., Indyk, P., Motwani, R., et al., 1999. Similarity search in high dimensions via  
1432 hashing, in: VLDB, pp. 518–529.
- 1433 Gletsos, M., Mougiakakou, S.G., Matsopoulos, G.K., Nikita, K.S., Nikita, A.S., Kelekis,  
1434 D., 2003. A computer-aided diagnostic system to characterize ct focal liver lesions: de-  
1435 sign and optimization of a neural network classifier. *IEEE Transactions on Information*  
1436 *Technology in Biomedicine* 7, 153–162.
- 1437 Gong, Y., Kumar, S., Verma, V., Lazebnik, S., 2012. Angular quantization-based binary  
1438 codes for fast similarity search, in: Advances in Neural Information Processing Systems,  
1439 pp. 1196–1204.
- 1440 Gong, Y., Lazebnik, S., 2011. Iterative quantization: A procrustean approach to learn-  
1441 ing binary codes, in: Computer Vision and Pattern Recognition (CVPR), 2011 IEEE  
1442 Conference on, IEEE. pp. 817–824.
- 1443 Gong, Y., Lazebnik, S., Gordo, A., Perronnin, F., 2013. Iterative quantization: A pro-  
1444 crustean approach to learning binary codes for large-scale image retrieval. *IEEE Trans-*  
1445 *actions on Pattern Analysis and Machine Intelligence* 35, 2916–2929.
- 1446 Gordo, A., Perronnin, F., Gong, Y., Lazebnik, S., 2014. Asymmetric distances for binary  
1447 embeddings. *IEEE Transactions on Pattern Analysis and Machine Intelligence* 36, 33–  
1448 47.
- 1449 Güld, M.O., Thies, C., Fischer, B., Lehmann, T.M., 2005. Content-based retrieval of  
1450 medical images by combining global features, in: Workshop of the Cross-Language  
1451 Evaluation Forum for European Languages, Springer. pp. 702–711.
- 1452 Gurcan, M.N., Boucheron, L.E., Can, A., Madabhushi, A., Rajpoot, N.M., Yener, B., 2009.  
1453 Histopathological image analysis: A review. *IEEE Reviews in Biomedical Engineering*  
1454 2, 147–171.
- 1455 Haas, S., Donner, R., Burner, A., Holzer, M., Langs, G., 2011. Superpixel-based interest  
1456 points for effective bags of visual words medical image retrieval, in: MICCAI Inter-  
1457 national Workshop on Medical Content-Based Retrieval for Clinical Decision Support,  
1458 Springer. pp. 58–68.

- 1459 He, J., Kumar, S., Chang, S.F., 2012. On the difficulty of nearest neighbor search, in:  
1460 Proceedings of the 29th international conference on machine learning (ICML-12), pp.  
1461 1127–1134.
- 1462 He, K., Zhang, X., Ren, S., Sun, J., 2015. Deep residual learning for image recognition.  
1463 arXiv preprint arXiv:1512.03385 .
- 1464 García Seco de Herrera, A., Schaer, R., Bromuri, S., Müller, H., 2016. Overview of the  
1465 ImageCLEF 2016 medical task, in: Working Notes of CLEF 2016 (Cross Language  
1466 Evaluation Forum), pp. 1–13.
- 1467 de Herrera, A.G.S., Kalpathy-Cramer, J., Demner-Fushman, D., Antani, S., Müller, H.,  
1468 2013. Overview of the imageclef 2013 medical tasks., in: CLEF (Working Notes).
- 1469 Hinton, G.E., Salakhutdinov, R.R., 2006. Reducing the dimensionality of data with neural  
1470 networks. *Science* 313, 504–507.
- 1471 Hofmann, T., 2001. Unsupervised learning by probabilistic latent semantic analysis. *Ma-  
1472 chine Learning* 42, 177–196.
- 1473 Hofmanninger, J., Langs, G., 2015. Mapping visual features to semantic profiles for re-  
1474 trieval in medical imaging, in: Proceedings of the IEEE Conference on Computer Vision  
1475 and Pattern Recognition, pp. 457–465.
- 1476 Hsieh, J., 2009. Computed tomography: principles, design, artifacts, and recent advances,  
1477 SPIE Bellingham, WA.
- 1478 Hsu, W., Long, L.R., Antani, S., et al., 2007. Spirs: a framework for content-based image  
1479 retrieval from large biomedical databases. *MedInfo* 12, 188–192.
- 1480 Huang, L.K., Yang, Q., Zheng, W.S., 2013. Online hashing., in: IJCAI, Citeseer.
- 1481 Hwang, K.H., Lee, H., Choi, D., 2012. Medical image retrieval: past and present. *Health-  
1482 care Informatics Research* 18, 3–9.
- 1483 ImageCLEF, . Image retrieval task of the conference and labs of the evaluation forum.  
1484 <http://www.imageclef.org/>. Accessed October 23, 2016.
- 1485 Institute, N.C., a. The cancer genome atlas. <https://tcga-data.nci.nih.gov/>. Ac-  
1486 cessed October 23, 2016.
- 1487 Institute, N.C., b. Genomic data commons. <https://gdc.cancer.gov/>. Accessed October  
1488 23, 2016.
- 1489 Institute, N.C., c. The national lung screening trial (nlst). [https://biometry.nci.nih.  
1490 gov/cdas/nlst/](https://biometry.nci.nih.gov/cdas/nlst/). Accessed March 23, 2017.
- 1491 IRMA, . Image retrieval in medical applications project. [http://ganymed.imib.  
rwth-aachen.de/irma/](http://ganymed.imib.<br/>1492 rwth-aachen.de/irma/). Accessed October 23, 2016.

- 1493 Jain, P., Kulis, B., Dhillon, I.S., Grauman, K., 2009. Online metric learning and fast  
1494 similarity search, in: *Advances in Neural Information Processing Systems*, pp. 761–768.
- 1495 Jain, P., Kulis, B., Grauman, K., 2008. Fast image search for learned metrics, in: *Com-  
1496 puter Vision and Pattern Recognition, 2008. CVPR 2008. IEEE Conference on, IEEE.*  
1497 pp. 1–8.
- 1498 Jiang, M., Zhang, S., Fang, R., Metaxas, D.N., 2015a. Leveraging coupled multi-index for  
1499 scalable retrieval of mammographic masses, in: *2015 IEEE 12th International Symposi-  
1500 sium on Biomedical Imaging (ISBI), IEEE.* pp. 276–280.
- 1501 Jiang, M., Zhang, S., Huang, J., Yang, L., Metaxas, D.N., 2015b. Joint kernel-based  
1502 supervised hashing for scalable histopathological image analysis, in: *International Con-  
1503 ference on Medical Image Computing and Computer-Assisted Intervention, Springer.*  
1504 pp. 366–373.
- 1505 Jiang, M., Zhang, S., Huang, J., Yang, L., Metaxas, D.N., 2016a. Scalable histopatho-  
1506 logical image analysis via supervised hashing with multiple features. *Medical Image  
1507 Analysis* 34, 3–12.
- 1508 Jiang, M., Zhang, S., Li, H., Metaxas, D.N., 2015c. Computer-aided diagnosis of mam-  
1509 mographic masses using scalable image retrieval. *IEEE Transactions on Biomedical  
1510 Engineering* 62, 783–792.
- 1511 Jiang, M., Zhang, S., Zheng, Y., Metaxas, D.N., 2016b. Mammographic mass segmenta-  
1512 tion with online learned shape and appearance priors, in: *International Conference on  
1513 Medical Image Computing and Computer-Assisted Intervention, Springer.* pp. 35–43.
- 1514 Jimenez-del-Toro, O., Hanbury, A., Langs, G., Foncubierta-Rodríguez, A., Müller, H.,  
1515 2015. Overview of the VISCERAL Retrieval Benchmark 2015, in: *Multimodal Retrieval  
1516 in the Medical Domain: First International Workshop, MRMD 2015, Vienna, Austria,  
1517 March 29, 2015, Revised Selected Papers, Springer.* pp. 115–123.
- 1518 Kahn, C.E., Carrino, J.A., Flynn, M.J., Peck, D.J., Horii, S.C., 2007. Dicom and radiology:  
1519 past, present, and future. *Journal of the American College of Radiology* 4, 652–657.
- 1520 Kalpathy-Cramer, J., de Herrera, A.G.S., Demner-Fushman, D., Antani, S., Bedrick, S.,  
1521 Müller, H., 2015. Evaluating performance of biomedical image retrieval systemsan  
1522 overview of the medical image retrieval task at imageclef 2004–2013. *Computerized  
1523 Medical Imaging and Graphics* 39, 55–61.
- 1524 Kalpathy-Cramer, J., Hersh, W., 2008. Effectiveness of global features for automatic med-  
1525 ical image classification and retrieval—the experiences of ohsu at imageclefmed. *Pattern  
1526 Recognition Letters* 29, 2032–2038.
- 1527 Kalpathy-Cramer, J., Müller, H., Bedrick, S., Eggel, I., de Herrera, A.G.S., Tsirikla, T.,  
1528 2011. Overview of the clef 2011 medical image classification and retrieval tasks., in:  
1529 CLEF (notebook papers/labs/workshop), pp. 97–112.



- 1530 Katouzian, A., Angelini, E.D., Carlier, S.G., Suri, J.S., Navab, N., Laine, A.F., 2012. A  
1531 state-of-the-art review on segmentation algorithms in intravascular ultrasound (ivus)  
1532 images. *IEEE Transactions on Information Technology in Biomedicine* 16, 823–834.
- 1533 Kim, H., El-Khamra, Y., Rodero, I., Jha, S., Parashar, M., 2011. Autonomic management  
1534 of application workflows on hybrid computing infrastructure. *Scientific Programming*  
1535 19, 75–89.
- 1536 Krizhevsky, A., Sutskever, I., Hinton, G.E., 2012. Imagenet classification with deep con-  
1537 volutional neural networks, in: *Advances in Neural Information Processing Systems*,  
1538 pp. 1097–1105.
- 1539 Kulis, B., Grauman, K., 2012. Kernelized locality-sensitive hashing. *IEEE Transactions*  
1540 *on Pattern Analysis and Machine Intelligence* 34, 1092–1104.
- 1541 Kulis, B., Jain, P., Grauman, K., 2009. Fast similarity search for learned metrics. *IEEE*  
1542 *Transactions on Pattern Analysis and Machine Intelligence* 31, 2143–2157.
- 1543 Kumar, A., Kim, J., Cai, W., Fulham, M., Feng, D., 2013. Content-based medical image  
1544 retrieval: a survey of applications to multidimensional and multimodality data. *Journal*  
1545 *of Digital Imaging* 26, 1025–1039.
- 1546 Kumar, V.S., Rutt, B., Kurc, T., Catalyurek, U., Saltz, J., Chow, S., Lamont, S., Martone,  
1547 M., 2006. Large image correction and warping in a cluster environment, in: *SC 2006*  
1548 *Conference, Proceedings of the ACM/IEEE, IEEE*. pp. 38–38.
- 1549 Lan, R., Zhou, Y., 2016. Medical image retrieval via histogram of compressed scattering  
1550 coefficients. *IEEE Journal of Biomedical and Health Informatics* .
- 1551 Langs, G., Hanbury, A., Menze, B., Müller, H., 2012. Visceral: Towards large data  
1552 in medical imaging challenges and directions, in: *MICCAI International Workshop on*  
1553 *Medical Content-Based Retrieval for Clinical Decision Support*, Springer. pp. 92–98.
- 1554 LeCun, Y., Bengio, Y., Hinton, G., 2015. Deep learning. *Nature* 521, 436–444.
- 1555 LeCun, Y., Bottou, L., Bengio, Y., Haffner, P., 1998. Gradient-based learning applied to  
1556 document recognition. *Proceedings of the IEEE* 86, 2278–2324.
- 1557 Lehmann, T.M., Gold, M., Thies, C., Fischer, B., Spitzer, K., Keysers, D., Ney, H.,  
1558 Kohnen, M., Schubert, H., Wein, B.B., 2004. Content-based image retrieval in medical  
1559 applications. *Methods of Information in Medicine* 43, 354–361.
- 1560 Leng, C., Wu, J., Cheng, J., Bai, X., Lu, H., 2015. Online sketching hashing, in: *Pro-*  
1561 *ceedings of the IEEE Conference on Computer Vision and Pattern Recognition*, pp.  
1562 2503–2511.
- 1563 Lewis, R., 2004. Medical phase contrast x-ray imaging: current status and future  
1564 prospects. *Physics in medicine and biology* 49, 3573–3584.

- 1565 Li, Q., Cai, W., Wang, X., Zhou, Y., Feng, D.D., Chen, M., 2014a. Medical image  
1566 classification with convolutional neural network, in: Control Automation Robotics &  
1567 Vision (ICARCV), 2014 13th International Conference on, IEEE. pp. 844–848.
- 1568 Li, R., Zhang, W., Suk, H.I., Wang, L., Li, J., Shen, D., Ji, S., 2014b. Deep learning based  
1569 imaging data completion for improved brain disease diagnosis, in: International Con-  
1570 ference on Medical Image Computing and Computer-Assisted Intervention, Springer.  
1571 pp. 305–312.
- 1572 Li, Z., Fang, R., Shen, F., Katouzian, A., Zhang, S., 2017a. Indexing and mining large-  
1573 scale neuron databases using maximum inner product search. *Pattern Recognition* 63,  
1574 680–688.
- 1575 Li, Z., Metaxas, D.N., Lu, A., Zhang, S., 2017b. Interactive exploration for continuously  
1576 expanding neuron databases. *Methods* 115, 100–109.
- 1577 Li, Z., Shen, F., Fang, R., Conjeti, S., Katouzian, A., Zhang, S., 2016. Maximum inner  
1578 product search for morphological retrieval of large-scale neuron data, in: *Biomedical*  
1579 *Imaging (ISBI)*, 2016 IEEE 13th International Symposium on, IEEE. pp. 602–606.
- 1580 Lichtman, J.W., Conchello, J.A., 2005. Fluorescence microscopy. *Nature Methods* 2,  
1581 910–919.
- 1582 Lim, J.H., Chevallet, J.P., 2005. Vismed: a visual vocabulary approach for medical image  
1583 indexing and retrieval, in: *Asia Information Retrieval Symposium*, Springer. pp. 84–96.
- 1584 Lin, T.Y., Maire, M., Belongie, S., Bourdev, L., Girshick, R., Hays, J., Perona, P., Ra-  
1585 manan, D., Zitnick, C.L., Dollar, P., 2014. Microsoft coco: Common objects in context.  
1586 arXiv preprint arXiv:1405.0312 .
- 1587 Lisin, D.A., Mattar, M.A., Blaschko, M.B., Learned-Miller, E.G., Benfield, M.C., 2005.  
1588 Combining local and global image features for object class recognition, in: 2005  
1589 IEEE Computer Society Conference on Computer Vision and Pattern Recognition  
1590 (CVPR'05)-Workshops, IEEE. pp. 47–47.
- 1591 Liu, H., Wang, R., Shan, S., Chen, X., 2016a. Deep supervised hashing for fast image  
1592 retrieval, in: *Proceedings of the IEEE Conference on Computer Vision and Pattern*  
1593 *Recognition*, pp. 2064–2072.
- 1594 Liu, J., Zhang, S., Liu, W., Deng, C., Zheng, Y., Metaxas, D.N., 2016b. Scalable mammo-  
1595 gram retrieval using composite anchor graph hashing with iterative quantization. *IEEE*  
1596 *Transactions on Circuits and Systems for Video Technology* PP, 1–11.
- 1597 Liu, J., Zhang, S., Liu, W., Zhang, X., Metaxas, D.N., 2014a. Scalable mammogram  
1598 retrieval using anchor graph hashing, in: 2014 IEEE 11th International Symposium on  
1599 Biomedical Imaging (ISBI), IEEE. pp. 898–901.

- 1600 Liu, W., Mu, C., Kumar, S., Chang, S.F., 2014b. Discrete graph hashing, in: Advances in  
1601 Neural Information Processing Systems, pp. 3419–3427.
- 1602 Liu, W., Wang, J., Ji, R., Jiang, Y.G., Chang, S.F., 2012. Supervised hashing with  
1603 kernels, in: Computer Vision and Pattern Recognition (CVPR), 2012 IEEE Conference  
1604 on, IEEE. pp. 2074–2081.
- 1605 Liu, W., Wang, J., Kumar, S., Chang, S.F., 2011. Hashing with graphs, in: Proceedings  
1606 of the 28th International Conference on Machine Learning (ICML-11), pp. 1–8.
- 1607 Liu, X., He, J., Lang, B., 2014c. Multiple feature kernel hashing for large-scale visual  
1608 search. *Pattern Recognition* 47, 748–757.
- 1609 Long, L.R., Antani, S., Deserno, T.M., Thoma, G.R., 2009. Content-based image re-  
1610 trieval in medicine: retrospective assessment, state of the art, and future directions.  
1611 *International Journal of Healthcare Information Systems and Informatics* 4, 1.
- 1612 Lowe, D.G., 2004. Distinctive image features from scale-invariant keypoints. *International*  
1613 *Journal of Computer Vision* 60, 91–110.
- 1614 Manjunath, B.S., Ma, W.Y., 1996. Texture features for browsing and retrieval of image  
1615 data. *IEEE Transactions on Pattern Analysis and Machine Intelligence* 18, 837–842.
- 1616 Markonis, D., Holzer, M., Baroz, F., De Castaneda, R.L.R., Boyer, C., Langs, G., Müller,  
1617 H., 2015a. User-oriented evaluation of a medical image retrieval system for radiologists.  
1618 *International journal of medical informatics* 84, 774–783.
- 1619 Markonis, D., Schaer, R., Eggel, I., Müller, H., Depeursinge, A., 2015b. Using mapreduce  
1620 for large-scale medical image analysis. *arXiv preprint arXiv:1510.06937* .
- 1621 May, M., 2010. A better lens on disease. *Scientific American* 302, 74–77.
- 1622 of Medicine, T.N.L., . Medpix. <https://medpix.nlm.nih.gov/home>. Accessed October  
1623 23, 2016.
- 1624 Mesbah, S., Conjeti, S., Kumaraswamy, A., Rautenberg, P., Navab, N., Katouzian, A.,  
1625 2015. Hashing forests for morphological search and retrieval in neuroscientific image  
1626 databases, in: *International Conference on Medical Image Computing and Computer-*  
1627 *Assisted Intervention*, Springer. pp. 135–143.
- 1628 Müller, H., Clough, P., Deselaers, T., Caputo, B., CLEF, I., 2010. Experimental evaluation  
1629 in visual information retrieval. *The Information Retrieval Series* 32.
- 1630 Müller, H., Deserno, T.M., 2010. Content-based medical image retrieval, in: *Biomedical*  
1631 *Image Processing*. Springer, pp. 471–494.
- 1632 Müller, H., de Herrera, A.G.S., Kalpathy-Cramer, J., Demner-Fushman, D., Antani, S.,  
1633 Eggel, I., 2012. Overview of the imageclef 2012 medical image retrieval and classification  
1634 tasks., in: *CLEF (online working notes/labs/workshop)*, pp. 1–16.

- 1635 Müller, H., Kalpathy-Cramer, J., Eggel, I., Bedrick, S., Radhouani, S., Bakke, B., Kahn,  
1636 C.E., Hersh, W., 2009. Overview of the clef 2009 medical image retrieval track, in:  
1637 Workshop of the Cross-Language Evaluation Forum for European Languages, Springer.  
1638 pp. 72–84.
- 1639 Müller, H., Menze, B., Langs, G., Montillo, A., Kelm, M., Zhang, S., Cai, W.T., Metaxas,  
1640 D., 2014. Overview of the 2014 workshop on medical computer vision algorithms for big  
1641 data (mcv 2014), in: International MICCAI Workshop on Medical Computer Vision,  
1642 Springer. pp. 3–10.
- 1643 Müller, H., Michoux, N., Bandon, D., Geissbuhler, A., 2004. A review of content-based  
1644 image retrieval systems in medical applications clinical benefits and future directions.  
1645 International Journal of Medical Informatics 73, 1–23.
- 1646 Muller, H., Muller, W., Marchand-Maillet, S., Pun, T., Squire, D.M., 2000. Strategies for  
1647 positive and negative relevance feedback in image retrieval, in: Pattern Recognition,  
1648 2000. Proceedings. 15th International Conference on, IEEE. pp. 1043–1046.
- 1649 Müller, H., Müller, W., Squire, D.M., Marchand-Maillet, S., Pun, T., 2001. Performance  
1650 evaluation in content-based image retrieval: overview and proposals. Pattern Recogni-  
1651 tion Letters 22, 593–601.
- 1652 Muller, H., Rosset, A., Vallee, J.P., Geissbuhler, A., 2004. Comparing features sets for  
1653 content-based image retrieval in a medical- case database, in: Proceedings of SPIE, pp.  
1654 99–109.
- 1655 Murala, S., Maheshwari, R., Balasubramanian, R., 2012. Directional binary wavelet pat-  
1656 terns for biomedical image indexing and retrieval. Journal of Medical Systems 36,  
1657 2865–2879.
- 1658 Nanni, L., Lumini, A., Brahnam, S., 2010. Local binary patterns variants as texture  
1659 descriptors for medical image analysis. Artificial Intelligence in Medicine 49, 117–125.
- 1660 NBIA, . National biomedical imaging archive. [https://imaging.nci.nih.gov/ncia/  
1661 login.jsf](https://imaging.nci.nih.gov/ncia/login.jsf). Accessed October 23, 2016.
- 1662 NCBI, . Pubmed central. <https://www.ncbi.nlm.nih.gov/pmc/>. Accessed March 23,  
1663 2017.
- 1664 NeuroMorpho, . Neuron morphological database. <http://neuromorpho.org/>. Accessed  
1665 October 23, 2016.
- 1666 Nister, D., Stewenius, H., 2006. Scalable recognition with a vocabulary tree, in: 2006  
1667 IEEE Computer Society Conference on Computer Vision and Pattern Recognition  
1668 (CVPR’06), IEEE. pp. 2161–2168.
- 1669 Norouzi, M., Fleet, D.J., Salakhutdinov, R.R., 2012. Hamming distance metric learning,  
1670 in: Advances in Neural Information Processing Systems, pp. 1061–1069.

- 1671 Ojala, T., Pietikäinen, M., Harwood, D., 1996. A comparative study of texture measures  
1672 with classification based on featured distributions. *Pattern Recognition* 29, 51–59.
- 1673 Oliva, A., Torralba, A., 2001. Modeling the shape of the scene: A holistic representation  
1674 of the spatial envelope. *International Journal of Computer Vision* 42, 145–175.
- 1675 Oliver, A., Freixenet, J., Marti, J., Pérez, E., Pont, J., Denton, E.R., Zwigelaar, R., 2010.  
1676 A review of automatic mass detection and segmentation in mammographic images.  
1677 *Medical Image Analysis* 14, 87–110.
- 1678 Peng, H., Ruan, Z., Long, F., Simpson, J.H., Myers, E.W., 2010. V3d enables real-time 3d  
1679 visualization and quantitative analysis of large-scale biological image data sets. *Nature*  
1680 *Biotechnology* 28, 348–353.
- 1681 Powers, D.M., 2011. Evaluation: from precision, recall and f-measure to roc, informedness,  
1682 markedness and correlation. *Journal of Machine Learning Technologies* 2, 37–63.
- 1683 Qi, X., Wang, D., Rodero, I., Diaz-Montes, J., Gensure, R.H., Xing, F., Zhong, H.,  
1684 Goodell, L., Parashar, M., Foran, D.J., et al., 2014. Content-based histopathology  
1685 image retrieval using cometcloud. *BMC Bioinformatics* 15, 1.
- 1686 Radhouani, S., Kalpathy-Cramer, J., Bedrick, S., Bakke, B., Hersh, W.R., 2009. Mul-  
1687 timodal medical image retrieval: Improving precision at imageclef 2009., in: *CLEF*  
1688 (Working Notes).
- 1689 Raginsky, M., Lazebnik, S., 2009. Locality-sensitive binary codes from shift-invariant  
1690 kernels, in: *Advances in Neural Information Processing Systems*, pp. 1509–1517.
- 1691 Rahman, M.M., Bhattacharya, P., Desai, B.C., 2007. A framework for medical image  
1692 retrieval using machine learning and statistical similarity matching techniques with  
1693 relevance feedback. *IEEE Transactions on Information Technology in Biomedicine* 11,  
1694 58–69.
- 1695 Rui, Y., Huang, T.S., Ortega, M., Mehrotra, S., 1998. Relevance feedback: a power tool for  
1696 interactive content-based image retrieval. *IEEE Transactions on Circuits and Systems*  
1697 *for Video Technology* 8, 644–655.
- 1698 Russakovsky, O., Deng, J., Su, H., Krause, J., Satheesh, S., Ma, S., Huang, Z., Karpathy,  
1699 A., Khosla, A., Bernstein, M., Berg, A.C., Fei-Fei, L., 2015. ImageNet Large Scale  
1700 Visual Recognition Challenge. *International Journal of Computer Vision (IJCV)* 115,  
1701 211–252. doi:[10.1007/s11263-015-0816-y](https://doi.org/10.1007/s11263-015-0816-y).
- 1702 Sahbi, H., Audibert, J.Y., Keriven, R., 2007. Graph-cut transducers for relevance feed-  
1703 back in content based image retrieval, in: *2007 IEEE 11th International Conference on*  
1704 *Computer Vision*, IEEE. pp. 1–8.
- 1705 Salakhutdinov, R., 2015. Learning deep generative models. *Annual Review of Statistics*  
1706 *and Its Application* 2, 361–385.

- 1707 Salton, G., Buckley, C., 1988. Term-weighting approaches in automatic text retrieval.  
1708 Information Processing & Management 24, 513–523.
- 1709 Schindelin, J., Arganda-Carreras, I., Frise, E., Kaynig, V., Longair, M., Pietzsch, T.,  
1710 Preibisch, S., Rueden, C., Saalfeld, S., Schmid, B., et al., 2012. Fiji: an open-source  
1711 platform for biological-image analysis. Nature Methods 9, 676–682.
- 1712 Schlegl, T., Ofner, J., Langs, G., 2014. Unsupervised pre-training across image domains  
1713 improves lung tissue classification, in: International MICCAI Workshop on Medical  
1714 Computer Vision, Springer. pp. 82–93.
- 1715 Semedo, D., Magalhães, J., . Novasearch at imageclefmed 2016 subfigure classification  
1716 task, in: CLEF2016 Working Notes. CEUR Workshop Proceedings, Évora, Portugal,  
1717 CEUR-WS.org (September 5-8 2016).
- 1718 Sertel, O., Kong, J., Catalyurek, U.V., Lozanski, G., Saltz, J.H., Gurcan, M.N., 2009.  
1719 Histopathological image analysis using model-based intermediate representations and  
1720 color texture: Follicular lymphoma grading. Journal of Signal Processing Systems 55,  
1721 169–183.
- 1722 Shen, D., Wu, G., Suk, H.I., 2016. Deep learning in medical image analysis. Annual  
1723 Review of Biomedical Engineering 19.
- 1724 Shen, F., Liu, W., Zhang, S., Yang, Y., Shen, H.T., 2015a. Learning binary codes for  
1725 maximum inner product search, in: 2015 IEEE International Conference on Computer  
1726 Vision (ICCV), IEEE. pp. 4148–4156.
- 1727 Shen, F., Shen, C., Liu, W., Tao Shen, H., 2015b. Supervised discrete hashing, in: Pro-  
1728 ceedings of the IEEE Conference on Computer Vision and Pattern Recognition, pp.  
1729 37–45.
- 1730 Shen, F., Shen, C., Shi, Q., van den Hengel, A., Tang, Z., Shen, H.T., 2015c. Hashing on  
1731 nonlinear manifolds. IEEE Transactions on Image Processing 24, 1839–1851.
- 1732 Shen, F., Shen, C., Shi, Q., Van Den Hengel, A., Tang, Z., 2013. Inductive hashing on  
1733 manifolds, in: Proceedings of the IEEE Conference on Computer Vision and Pattern  
1734 Recognition, pp. 1562–1569.
- 1735 Shen, W., Zhou, M., Yang, F., Yang, C., Tian, J., 2015d. Multi-scale convolutional neural  
1736 networks for lung nodule classification, in: International Conference on Information  
1737 Processing in Medical Imaging, Springer. pp. 588–599.
- 1738 Shin, H.C., Orton, M.R., Collins, D.J., Doran, S.J., Leach, M.O., 2013. Stacked autoen-  
1739 coders for unsupervised feature learning and multiple organ detection in a pilot study  
1740 using 4d patient data. IEEE Transactions on Pattern Analysis and Machine Intelligence  
1741 35, 1930–1943.

- 1742 Shin, H.C., Roth, H.R., Gao, M., Lu, L., Xu, Z., Nogues, I., Yao, J., Mollura, D., Sum-  
1743 mers, R.M., 2016. Deep convolutional neural networks for computer-aided detection:  
1744 Cnn architectures, dataset characteristics and transfer learning. *IEEE Transactions on*  
1745 *Medical Imaging* 35, 1285–1298.
- 1746 Siemens, . Great growth potential for medical imaging systems. <http://www.siemens.com/innovation/en/home/pictures-of-the-future/health-and-well-being/medical-imaging-facts-and-forecasts.html>. Accessed October 23, 2016.
- 1749 Siggelkow, S., 2002. Feature histograms for content-based image retrieval. Ph.D. thesis.  
1750 Universität Freiburg.
- 1751 Simonyan, K., Zisserman, A., 2014. Very deep convolutional networks for large-scale image  
1752 recognition. arXiv preprint arXiv:1409.1556 .
- 1753 Simpson, M.S., You, D., Rahman, M.M., Demner-Fushman, D., Antani, S., Thoma, G.R.,  
1754 2012. Iti’s participation in the imageclef 2012 medical retrieval and classification tasks.,  
1755 in: *CLEF (Online Working Notes/Labs/Workshop)*.
- 1756 Sivic, J., Zisserman, A., 2003. Video google: A text retrieval approach to object matching  
1757 in videos, in: *Computer Vision, 2003. Proceedings. Ninth IEEE International Confer-*  
1758 *ence on, IEEE*. pp. 1470–1477.
- 1759 Slichter, C.P., 2013. Principles of magnetic resonance. volume 1. Springer Science &  
1760 Business Media.
- 1761 Smolensky, P., 1986. Information processing in dynamical systems: foundations of har-  
1762 mony theory, in: *Parallel Distributed Processing: Explorations in the Microstructure*  
1763 *of Cognition*, vol. 1, MIT Press. pp. 194–281.
- 1764 Society, A.C., 2013. Breast Cancer Facts & Figures 2013-2014. volume 1. American Cancer  
1765 Society.
- 1766 Song, L., Liu, X., Ma, L., Zhou, C., Zhao, X., Zhao, Y., 2012. Using hog-lbp features and  
1767 mmp learning to recognize imaging signs of lung lesions, in: *Computer-Based Medical*  
1768 *Systems (CBMS), 2012 25th International Symposium on, IEEE*. pp. 1–4.
- 1769 of South Florida, U., . Usf digital mammography homepage. <http://marathon.csee.usf.edu/Mammography/>. Accessed October 23, 2016.
- 1771 of Southern California, U., . Alzheimer’s disease neuroimaging initiative. <http://adni.loni.usc.edu/>. Accessed October 23, 2016.
- 1773 Srivastava, N., Hinton, G.E., Krizhevsky, A., Sutskever, I., Salakhutdinov, R., 2014.  
1774 Dropout: a simple way to prevent neural networks from overfitting. *Journal of Ma-*  
1775 *chine Learning Research* 15, 1929–1958.

- 1776 Stricker, M.A., Orengo, M., 1995. Similarity of color images, in: IS&T/SPIE's Symposium  
1777 on Electronic Imaging: Science & Technology, International Society for Optics and  
1778 Photonics. pp. 381–392.
- 1779 Szabo, T.L., 2004. Diagnostic ultrasound imaging: inside out. Academic Press.
- 1780 Sze-To, A., Tizhoosh, H.R., Wong, A.K., 2016. Binary codes for tagging x-ray images via  
1781 deep de-noising autoencoders, in: Neural Networks (IJCNN), 2016 International Joint  
1782 Conference on, IEEE. pp. 2864–2871.
- 1783 Szegedy, C., Liu, W., Jia, Y., Sermanet, P., Reed, S., Anguelov, D., Erhan, D., Vanhoucke,  
1784 V., Rabinovich, A., 2015. Going deeper with convolutions, in: Proceedings of the IEEE  
1785 Conference on Computer Vision and Pattern Recognition, pp. 1–9.
- 1786 Tabesh, A., Teverovskiy, M., Pang, H.Y., Kumar, V.P., Verbel, D., Kotsianti, A., Saidi,  
1787 O., 2007. Multifeature prostate cancer diagnosis and gleason grading of histological  
1788 images. IEEE Transactions on Medical Imaging 26, 1366–1378.
- 1789 Tamura, H., Mori, S., Yamawaki, T., 1978. Textural features corresponding to visual  
1790 perception. IEEE Transactions on Systems, Man, and Cybernetics 8, 460–473.
- 1791 Tang, L.H.Y., Hanka, R., Ip, H.H.S., 1999. A review of intelligent content-based indexing  
1792 and browsing of medical images. HIJ 5, 40–49.
- 1793 TCIA, . The cancer imaging archive. <http://www.cancerimagingarchive.net/>. Ac-  
1794 cessed October 23, 2016.
- 1795 Tian, G., Fu, H., Feng, D.D., 2008. Automatic medical image categorization and anno-  
1796 tation using lbp and mpeg-7 edge histograms, in: 2008 International Conference on  
1797 Information Technology and Applications in Biomedicine, IEEE. pp. 51–53.
- 1798 Jiménez-del Toro, O.A., Cirujeda, P., Cid, Y.D., Müller, H., 2015. Radlex terms and local  
1799 texture features for multimodal medical case retrieval, in: Multimodal Retrieval in the  
1800 Medical Domain. Springer, pp. 144–152.
- 1801 del Toro, O.A.J., Foncubierta-Rodriguez, A., Gómez, M.I.V., Müller, H., Depeursinge, A.,  
1802 2013. Epileptogenic lesion quantification in mri using contralateral 3d texture com-  
1803 parisons, in: International Conference on Medical Image Computing and Computer-  
1804 Assisted Intervention, Springer. pp. 353–360.
- 1805 Tourassi, G.D., Harrawood, B., Singh, S., Lo, J.Y., Floyd, C.E., 2007. Evaluation of  
1806 information-theoretic similarity measures for content-based retrieval and detection of  
1807 masses in mammograms. Medical Physics 34, 140–150.
- 1808 Trzcinski, T., Lepetit, V., 2012. Efficient discriminative projections for compact binary  
1809 descriptors, in: European Conference on Computer Vision, Springer. pp. 228–242.



- 1810 Unay, D., Ekin, A., 2011. Dementia diagnosis using similar and dissimilar retrieval items,  
1811 in: 2011 IEEE International Symposium on Biomedical Imaging: From Nano to Macro,  
1812 IEEE. pp. 1889–1892.
- 1813 Vincent, P., Larochelle, H., Lajoie, I., Bengio, Y., Manzagol, P.A., 2010. Stacked denoising  
1814 autoencoders: Learning useful representations in a deep network with a local denoising  
1815 criterion. *Journal of Machine Learning Research* 11, 3371–3408.
- 1816 VISCERAL, . Visual concept extraction challenge in radiology. [http://www.visceral.  
1817 eu/benchmarks/retrieval2-benchmark/](http://www.visceral.eu/benchmarks/retrieval2-benchmark/). Accessed October 23, 2016.
- 1818 Wan, J., Wang, D., Hoi, S.C.H., Wu, P., Zhu, J., Zhang, Y., Li, J., 2014. Deep learning  
1819 for content-based image retrieval: A comprehensive study, in: *Proceedings of the 22nd  
1820 ACM international conference on Multimedia*, ACM. pp. 157–166.
- 1821 Wan, Y., Long, F., Qu, L., Xiao, H., Hawrylycz, M., Myers, E.W., Peng, H., 2015. Blast-  
1822 neuron for automated comparison, retrieval and clustering of 3d neuron morphologies.  
1823 *Neuroinformatics* 13, 487–499.
- 1824 Wang, J., Kumar, S., Chang, S.F., 2012. Semi-supervised hashing for large-scale search.  
1825 *IEEE Transactions on Pattern Analysis and Machine Intelligence* 34, 2393–2406.
- 1826 Wang, J., Li, Y., Zhang, Y., Wang, C., Xie, H., Chen, G., Gao, X., 2011a. Bag-of-features  
1827 based medical image retrieval via multiple assignment and visual words weighting. *IEEE  
1828 Transactions on Medical Imaging* 30, 1996–2011.
- 1829 Wang, J., Liu, W., Kumar, S., Chang, S.F., 2016. Learning to hash for indexing big dataa  
1830 survey. *Proceedings of the IEEE* 104, 34–57.
- 1831 Wang, J., Xiao, J., Lin, W., Luo, C., 2015. Discriminative and generative vocabulary  
1832 tree: With application to vein image authentication and recognition. *Image and Vision  
1833 Computing* 34, 51–62.
- 1834 Wang, X., Yang, M., Cour, T., Zhu, S., Yu, K., Han, T.X., 2011b. Contextual weighting for  
1835 vocabulary tree based image retrieval, in: *2011 International Conference on Computer  
1836 Vision*, IEEE. pp. 209–216.
- 1837 Weiss, Y., Torralba, A., Fergus, R., 2009. Spectral hashing, in: *Advances in Neural  
1838 Information Processing Systems*, pp. 1753–1760.
- 1839 Wolterink, J.M., Leiner, T., Viergever, M.A., Išgum, I., 2015. Automatic coronary cal-  
1840 cium scoring in cardiac ct angiography using convolutional neural networks, in: *Internation-  
1841 al Conference on Medical Image Computing and Computer-Assisted Intervention*,  
1842 Springer. pp. 589–596.
- 1843 Wu, G., Kim, M., Wang, Q., Gao, Y., Liao, S., Shen, D., 2013. Unsupervised deep feature  
1844 learning for deformable registration of mr brain images, in: *International Conference on  
1845 Medical Image Computing and Computer-Assisted Intervention*, Springer. pp. 649–656.

- 1846 Wu, G., Kim, M., Wang, Q., Munsell, B.C., Shen, D., 2016. Scalable high-performance  
1847 image registration framework by unsupervised deep feature representations learning.  
1848 IEEE Transactions on Biomedical Engineering 63, 1505–1516.
- 1849 Xing, F., Yang, L., 2016. Robust nucleus/cell detection and segmentation in digital pathol-  
1850 ogy and microscopy images: a comprehensive review. IEEE Reviews in Biomedical  
1851 Engineering 9, 234–263.
- 1852 Xue, Z., Long, L.R., Antani, S., Jeronimo, J., Thoma, G.R., 2008. A web-accessible  
1853 content-based cervicographic image retrieval system, in: Medical Imaging, International  
1854 Society for Optics and Photonics. pp. 691907–691907.
- 1855 Yu, G., Yuan, J., 2014. Scalable forest hashing for fast similarity search, in: Multimedia  
1856 and Expo (ICME), 2014 IEEE International Conference on, IEEE. pp. 1–6.
- 1857 Yu, X., Zhang, S., Liu, B., Zhong, L., Metaxas, D., 2013. Large scale medical image search  
1858 via unsupervised pca hashing, in: Proceedings of the IEEE Conference on Computer  
1859 Vision and Pattern Recognition Workshops, pp. 393–398.
- 1860 Zhang, F., Song, Y., Cai, W., Depeursinge, A., Müller, H., 2015a. Usyd/hes-so in the  
1861 visceral retrieval benchmark, in: Multimodal Retrieval in the Medical Domain. Springer,  
1862 pp. 139–143.
- 1863 Zhang, S., Metaxas, D., 2016. Large-scale medical image analytics: Recent methodologies,  
1864 applications and future directions. Medical Image Analysis 33, 98–101.
- 1865 Zhang, S., Yang, M., Cour, T., Yu, K., Metaxas, D.N., 2012. Query specific fusion for  
1866 image retrieval, in: Computer Vision–ECCV 2012. Springer, pp. 660–673.
- 1867 Zhang, S., Yang, M., Cour, T., Yu, K., Metaxas, D.N., 2015b. Query specific rank fusion  
1868 for image retrieval. IEEE Transactions on Pattern Analysis and Machine Intelligence  
1869 37, 803–815.
- 1870 Zhang, X., Dou, H., Ju, T., Xu, J., Zhang, S., 2016a. Fusing heterogeneous features  
1871 from stacked sparse autoencoder for histopathological image analysis. IEEE Journal of  
1872 Biomedical and Health Informatics 20, 1377–1383.
- 1873 Zhang, X., Liu, W., Dundar, M., Badve, S., Zhang, S., 2015c. Towards large-scale  
1874 histopathological image analysis: Hashing-based image retrieval. IEEE Transactions  
1875 on Medical Imaging 34, 496–506.
- 1876 Zhang, X., Liu, W., Zhang, S., 2014. Mining histopathological images via hashing-based  
1877 scalable image retrieval, in: 2014 IEEE 11th International Symposium on Biomedical  
1878 Imaging (ISBI), IEEE. pp. 1111–1114.
- 1879 Zhang, X., Xing, F., Su, H., Yang, L., Zhang, S., 2015d. High-throughput histopathological  
1880 image analysis via robust cell segmentation and hashing. Medical Image Analysis 26,  
1881 306–315.

- 1882 Zhang, X., Zhou, F., Lin, Y., Zhang, S., 2016b. Embedding label structures for fine-  
1883 grained feature representation, in: The IEEE Conference on Computer Vision and  
1884 Pattern Recognition (CVPR).
- 1885 Zhou, J., Feng, C., Liu, X., Tang, J., 2012. A texture features based medical image retrieval  
1886 system for breast cancer, in: Computing and Convergence Technology (ICCCT), 2012  
1887 7th International Conference on, IEEE. pp. 1010–1015.